

1 **Title: A genome-wide screen reveals that reducing mitochondrial DNA polymerase can**
2 **promote elimination of deleterious mitochondrial mutations**

3
4 Ason C.-Y. Chiang^{1,2}, Eleanor McCartney^{1,2}, Patrick H O'Farrell³, Hansong Ma^{1,2}

5
6 ¹Wellcome Trust/Cancer Research UK Gurdon Institute, Tennis Court Road, Cambridge CB2
7 1QN, UK

8 ²Department of Genetics, University of Cambridge, Downing Street, Cambridge CB2 3EH, UK

9 ³Department of Biochemistry and Biophysics, University of California, San Francisco, CA94143,
10 USA

11
12 Lead Contact: Hansong Ma (hm555@cam.ac.uk)

13 Additional Corresponding Author: Patrick H O'Farrell (ofarrell@cgl.ucsf.edu)

14
15
16
17 **Summary**

18
19 A mutant mitochondrial genome arising amid the pool of mitochondrial genomes within a cell
20 must compete with existing genomes to survive to the next generation. Even weak selective
21 forces can bias transmission of one genome over another to impact the inheritance of
22 mitochondrial diseases and guide the evolution of mitochondrial DNA (mtDNA). Studies in
23 several systems suggested that purifying selection in the female germline reduces transmission
24 of detrimental mitochondrial mutations[1-7]. In contrast, some selfish genomes can take over
25 despite a cost to host fitness[8-13]. Within individuals, the outcome of competition is therefore
26 influenced by multiple selective forces. The nuclear genome, which encodes most proteins
27 within mitochondria, and all external regulators of mitochondrial biogenesis and dynamics can
28 influence the competition between mitochondrial genomes[14-18]. Yet, little is known about how
29 this works. Previously, we established a *Drosophila* line transmitting two mitochondrial genomes
30 in a stable ratio enforced by purifying selection benefiting one genome and a selfish advantage
31 favouring the other[8]. To find nuclear genes that impact mtDNA competition, here we screened
32 heterozygous deletions tiling ~70% of the euchromatic regions and examined their influence on
33 this ratio. This genome-wide screen detected many nuclear modifiers of this ratio and identified
34 one as the catalytic subunit of mtDNA polymerase gene (*POLG*), *tam*. A reduced dose
35 of *tam* drove elimination of defective mitochondrial genomes. This study suggests that our
36 approach will uncover targets for interventions that would block propagation of pathogenic
37 mitochondrial mutations.

Results and Discussion

Drosophila melanogaster tolerates heterozygous deletions well, and collections of chromosomal deletions (i.e. deficiencies) tiling 98% of the euchromatic genome have been developed for genetic screening purposes[19,20]. To uncover nuclear regions that regulate mtDNA competition, we performed a deficiency screen on a heteroplasmic line that stably transmits two genomes: a functional mtDNA from *Drosophila yakuba* (*mt:yak*) and a temperature sensitive lethal genome harbouring two mutations, *mt:ND2^{del1}+Col^{T300I}* from *D. melanogaster* (Figure 1A)[8]. Previously, we showed that the *D. melanogaster* genome has a selfish transmission advantage, whereas *mt:yak* is favoured by purifying selection as it provides the functional *mt:Col*. The two opposing selections are balanced so that the heteroplasmic ratio (~5% *mt:yak* to ~95% *mt:ND2^{del1}+Col^{T300I}*) was stable for over 70 generations at the restrictive temperature (29 °C) of the *mt:ND2^{del1}+Col^{T300I}* genome (Figure 1A). We reasoned that a balance of two selective forces would be very sensitive to perturbation. Perhaps just a change in the gene dose of nuclear genes modulating competition would alter the ratio of mitochondrial genomes.

For the screen, 339 deletion chromosomes covering most of chromosome II and III were introduced into the heteroplasmic flies (Table S1). Sixty-three crosses produced no or few progeny carrying the deletion (Table S1). While it is likely that the lethality for some of the crosses was due to an inability to maintain the functional *mt:yak* genome, here we focus only on the 276 lines that produced progeny; in these, we measured the *mt:yak* percentage in adult males one generation after the deletion was introduced (i.e. generation 2, Figure 1B). Five lines had a substantially higher percentage of *mt:yak* ($\geq 10\%$), while thirty-three lines had a lower percentage ($\leq 2\%$) (Table S2 & S3). More than 10% of the tested lines changed the *mt:yak* percentage, leading us to conclude that multiple nuclear factors directly or indirectly regulate competition between mitochondrial genomes.

Of the 38 deficiencies that altered the *mt:yak* percentage, the two (BSC252 and BSC812) causing the largest increase (~28%) partially overlap (Table S3, Figure 1C&D). This suggests that a locus lying in the 60 kb region of the 2nd chromosome removed by both deletions is responsible for the observed phenotype (Figure 1D). Consistent with a common defect, both deletions caused a progressive and parallel rise in *mt:yak* over multiple generations until it reached 100% at generation 5 (Figure 1C). To produce this progressive heritable rise, these deletions must give *mt:yak* a selective advantage in the germline allowing accumulation in each generation. To confirm and further narrow down the responsible region, we tested two more deletions: Exel7059 (lacks the entire 60 kb region) and FDD-0428643 (only lacks the left 15 kb segment of the 60 kb region). Both gave the same increase in *mt:yak* (Figure S1A). This confined our candidates to eight genes, including four with known mitochondrial functions: mtDNA polymerase catalytic subunit *POLG* (*tam*), mtDNA polymerase accessory subunit *POLG2* (*pol* γ - β), glutamyl tRNA-aminotransferase *GatC* and mitochondrial ribosomal protein *mRpS23* (Figure S1B).

To investigate whether *pol* γ - β and its neighbouring and co-transcribed gene *GatC* play a role in regulating mtDNA transmission, we generated loss-of-function mutants via CRISPR/Cas9-based editing (Figure S2). Heterozygous mutants of *pol* γ - β and *GatC* did not alter *mt:yak* percentages, suggesting neither were responsible for the changes in the heteroplasmy ratio (Figure 2A). We then tested three *tam* mutants: two classical mutations *tam*³ and *tam*⁴, which contain small deletions that shift the reading frame[21], and *tam*^{KO}, which removes the entire coding region including the UTRs[22]. Heterozygosity for each of these *tam* mutations increased the *mt:yak* percentage just as observed with the four deficiencies (Figure 2B). By generation 5, *mt:yak* took over. To test reversibility of the effect, a wild-type *tam* genotype was restored in

89 some flies having a residual ~20% of *mt:ND2^{del1}+Col^{T3001}* at generation 4 and followed over
90 subsequent generations (Figure 2B). In these flies, selection reversed its course and *mt:yak*
91 declined. After four generations, *mt:yak* levels re-balanced at 5%. Of note, in accord with the
92 gene dose, the mRNA level of *tam* is halved in the deletion lines (Figure S3A). Despite the
93 dramatic shifts in the relative abundance of the two genomes, only minor fluctuations in total
94 copy number were detected in the newly laid eggs and adult flies (Figure S3B, also shown
95 in[22]). We conclude that removing one functional genomic copy of *tam* but not *pol γ-β* or *GatC*
96 increased the *mt:yak* percentage in the given nuclear background.

97
98 We were somewhat surprised that the dose of the gene encoding the catalytic subunit of POLG
99 modified competition while the dose of the essential accessory subunit did not. To pursue this
100 further, we tested other genes involved in mtDNA replication (*twk*, *mtSSB*, *TFAM* and *Top3α*)
101 and did not detect modification of the heteroplasmic ratio in a manner dependent on the dose of
102 these genes (Figure S3C). Thus, at least in the context of our screen, the input of *tam* appears
103 to be relatively specific among replication functions.

104
105 To test whether the influence of *tam* dose on mtDNA competition extended beyond the specific
106 mtDNA pair used in the screen, we examined a different pairing of mitochondrial genomes. We
107 previously showed that when the *mt:ND2^{del1}+Col^{T3001}* genome is paired with a distantly-related *D.*
108 *melanogaster* mitochondrial genome *mt:ATP6[1]*, the temperature sensitive mutant genome
109 exhibits such a powerful selfish advantage that it overrides the constraint of purifying selection;
110 the mutant genome replaced the complementing *mt:ATP6[1]* over a few generations, leading to
111 the death of the entire lineage at 29 °C[23]. We re-established two independent lineages of this
112 unstable heteroplasmy, and *mt:ND2^{del1}+Col^{T3001}* percentages rose rapidly as expected (Figure
113 2C). Before the demise of the stock, we removed one copy of functional *tam* by introducing
114 chromosomes bearing the *tam³* or *tam⁴* mutation in flies at generation 4, which still had ~10%
115 *mt:ATP6[1]*. Instead of observing a continued decline of *mt:ATP6[1]* as in control flies,
116 *mt:ATP6[1]* percentages increased over successive generations in the two lines with introduced
117 *tam* mutations (Figure 2C). After five generations, *mt:ATP6[1]* reached 100%. We conclude that
118 reducing the gene dose of *tam* can increase the transmission of a distinct functional
119 mitochondrial genome.

120
121 Since mtDNA competition in the two tested heteroplasmic lines is influenced by both purifying
122 and selfish selection, the effect of *tam* dose could be due to enhancement of purifying selection
123 to benefit the functional genome (*mt:yak* or *mt:ATP6[1]*), or diminution of the selfish
124 transmission advantage of *mt:ND2^{del1}+Col^{T3001}*, or both. To address this, we transferred the
125 *mt:yak/mt:ND2^{del1}+Col^{T3001}* lines to a lower temperature (22 °C) where purifying selection against
126 the *mt:ND2^{del1}+Col^{T3001}* is greatly diminished because of improved function of the mutant[5]. At
127 this temperature, selfish selection dominates the competition, and *mt:yak* percentage declined
128 and became undetectable in two generations in control fly groups (Figure 3A, also described
129 in[8]). When *tam* was heterozygous, *mt:yak* declined just as it did in control flies (Figure 3A).
130 Thus, at least in this experimental context, the dose of *tam* has little or no effect when selfish
131 selection has the dominant influence. Either *tam* dose does not act on selfish selection, or *tam*
132 dose is unable to act on selfish selection at this lower temperature.

133
134 Next, we examined the effect of *tam* dose in a heteroplasmic combination where only purifying
135 selection affects mtDNA competition. We previously showed that when a *mt:ND2^{del1}* genome
136 was paired with a *mt:Col^{T3001}* genome, the *mt:ND2^{del1}* steadily outcompetes the *mt:Col^{T3001}* due to
137 a difference in the oxidative phosphorylation (OXPHOS) function at 29 °C[5]. These two
138 genomes share the same non-coding region, and differ only by mutations in *mt:ND2* and *mt:Col*,
139 so there is no selfish selection involved. We found that in flies where *tam* dose was reduced, the

140 decline of *mt:Col^{T300I}* was accelerated (Figure 3B), suggesting that the decreased dose of *tam*
141 enhances purifying selection. To further test whether *tam* dose acts only on *mt:Col^{T300I}* or is only
142 manifested at 29 °C, we generated another heteroplasmic line where the *mt:ND2^{del1}* mutant was
143 paired with the wild-type mtDNA and we followed the heteroplasmy dynamics at 25 °C. The
144 *mt:ND2^{del1}* allele is slightly compromised for OXPHOS function and it is slowly displaced by the
145 wild type due to a weak purifying selection[5] (Figure 3C). In lines with only one functional
146 genomic copy of *tam*, the wild-type mtDNA took over faster (Figure 3C). Thus, reducing *tam*
147 acts to enhance two distinct examples of purifying selection. In each of these combinations of
148 mitochondrial genomes, it appears that reduction of *tam* favours transmission of functional
149 mtDNA, thereby promoting purifying selection.

150
151 For all the experiments described above, genetic crosses were designed to minimise nuclear
152 background differences and all tested deletions and mutations were heterozygous with a
153 balancer chromosome (*CyO* for all presented data and *TM6B* for the 3rd chromosome
154 deficiencies, see Figure 1B and STAR Methods). However, this left open the possibility that the
155 dose effect on heteroplasmy dynamics we observed for *tam* is specific for the given nuclear
156 background. To test whether this is the case, we altered the crossing scheme and examined the
157 consequence of *tam* heterozygosity with different second chromosomes instead of testing
158 mutations as heterozygotes with a standard balancer chromosome *CyO*. We found that, when
159 chromosomes unrelated to the *CyO* balancer were used, the dose of *tam* had only negligible
160 effect on the *mt:yak* percentage (Figure 4A). This suggests that the *CyO* chromosome carries
161 one or more polymorphisms that synergize with the *tam* dose to create the observed phenotype.
162 We hypothesized that the *CyO* balancer provided less *tam* function than other chromosomes
163 (hypomorphic for *tam*). Such behaviour might be attributed to either direct changes in the *tam*
164 sequence or other modifying mutations that reduce the functional output of Tam. We tested
165 various balancer chromosomes with related origins but different polymorphisms in the *tam*
166 sequence. While heterozygosity for *tam* gave a phenotype with all of these balancers, the
167 strength of the phenotype varied. This variation combined with sequences of *tam* from these
168 balancers (Figure S4A) and a test of *tam* expression from *CyO* (Figure S4B) suggests that the
169 modification is complex and might either be caused by diverse polymorphisms associated with
170 *tam* on the balancer or unrelated modifiers.

171
172 To avoid the complicated genetic interactions with the *CyO* balancer, we tested whether a more
173 substantial change in *tam* alone might be sufficient to modulate mtDNA competition. We used
174 CRISPR/Cas9-based mutagenesis to isolate mutations missing a single amino acid in the highly
175 conserved exonuclease domain of *tam* (*tam^{A262Y}* and *tam^{A263D}*) (Figure S2). These alleles are
176 homozygous viable, and also transheterozygous viable with *tam³*, *tam⁴* and *tam^{KO}*. We found
177 that after introducing two copies of *tam^{A262Y}* or *tam^{A263D}* in the *mt:yak/mt:ND2^{del1}+Col^{T300I}* line, the
178 *mt:yak* percentage increased to over 75% at generation 2. Similarly, the *mt:yak* percentage in
179 trans-heterozygous *tam/tam^{A262Y}* or *tam/tam^{A263D}* increased to over 70% at generation 2 (Figure
180 4B, Figure S4C). These data suggest that compromising *tam* function alone is sufficient to
181 modify the competition between mitochondrial genomes, but Tam function probably needs to be
182 reduced to less than 50%. Additionally, we analysed the consequence of an increase in *tam*
183 dose by following flies with two extra copies of *tam* (BacTam). Over a few generations at 29 °C,
184 the percentage of *mt:yak* fell from 6% to 2% in BacTam background (Figure 4C). All the above
185 data suggest that altering *tam* functional output alone is sufficient to influence the transmission
186 of the detrimental mitochondrial genomes.

187
188 Our findings show that the balance that maintains mitochondrial genomes in a stable
189 heteroplasmic state is precarious and modified by many genetic loci and that the shift in function
190 of one of these, *tam*, can drive the elimination of a detrimental mitochondrial mutation that was

191 otherwise stably inherited for many generations. The discovery that the gene involved encodes
192 the mtDNA polymerase suggests a connection with replication of the genomes, but the genetic
193 analysis reported here does not directly reveal the mechanism. It is tempting to speculate that
194 reducing Tam activity might favour the replication of the diverged *mt:yak* genome, but no such
195 favouritism was observed when temperature was reduced to minimise the functional difference
196 between *mt:yak* and the *mt:ND2^{del1}+CoI^{T300I}* genome. Furthermore, at 25 °C, the lower dose of
197 *tam* still favoured the functional genome when two *D. melanogaster* mitochondrial genomes
198 were pitted against each other (Figure 3C). This suggests that the differential effect of *tam* dose
199 impacts the effectiveness of purifying selection. While speculative, such an effect might be
200 explained by the involvement of Tam in a newly advanced quality control mechanism. Recently,
201 Zhang et al. showed that PINK1, a kinase sensitive to mitochondrial potential, is selectively
202 stabilized on the surface of mitochondria enriched for mutant genomes[24]. They further showed
203 that PINK1 phosphorylates Larp to inhibit local translation of nuclear-encoded mitochondrial
204 proteins on the surface of the unfit mitochondria. Tam was one of the factors whose expression
205 was dramatically reduced by this signalling pathway. They proposed that reduced translation
206 starves unfit mitochondria of nuclear encoded replication factors. Accordingly, Tam could be a
207 key factor limiting replication in unfit mitochondria when it falls below a certain threshold. A
208 reduction in the dose could promote the action of this system by making it easier to reach the
209 threshold that starves the unfit mitochondria of this limiting factor. However, cell biological and
210 disease phenotypes of *POLG* mutations are diverse, suggesting the existence of alternative
211 possible explanations for how dose change can impact the balance of heteroplasmic
212 genomes[25-28].

213
214 Regardless of mechanism, our genetic findings reveal that nuclear factors can govern the
215 competition between mitochondrial genomes, and we identify Tam as one of the influential
216 nuclear factors. We detected numerous nuclear loci that impact the competition between
217 mitochondrial genomes, suggesting that multiple pathways influence the selective forces
218 defining the outcome of competition. Perhaps reflecting complex inputs, the magnitude of the
219 impact of *tam* gene dose differs strikingly in different genetic backgrounds. In the two examples
220 where diverged mitochondrial genomes are differently favoured by selfish and purifying
221 selection, reduction of *tam* gene dose completely reverses the outcome of the competition such
222 that the winner becomes the loser and is eliminated (Figure 2B&C). This outcome seems out of
223 proportion with the more subtle shifts in the strength of purifying selection assessed in other
224 heteroplasmic backgrounds (Figure 3B&C). Perhaps as yet unappreciated differences in the
225 interaction of Tam with the much-altered regulatory regions of these competing genomes
226 increases the sensitivity to *tam* dose in these competitions.

227
228 In conclusion, the genetic approach we have used here has the potential of defining in some
229 detail the largely unknown rules of nuclear management of mtDNA transmission (e.g. [14-18]).
230 The pervasive impact of a change in the level of mtDNA polymerase catalytic subunit shows the
231 potency of the nuclear influence on the success of mitochondrial genomes, a factor that would
232 impact the inheritance of heteroplasmic mitochondrial disease traits. The large number of loci
233 that influence selection suggests that nuclear management of mitochondrial evolution is deeply
234 entrenched. We propose that it has played a role throughout eukaryotic evolution in taming and
235 subjugating the genome of an infecting microbe to adopt its current role. Since many
236 mitochondrial diseases are carried in heteroplasmy, the extensive nuclear inputs might identify
237 pharmacologically accessible pathways whose manipulation could provide clinical benefit.

238 **Acknowledgments**

239 We would like to thank Dr Hong Xu (National Heart, Lung and Blood Institute) for generously
240 sharing the BacTam flies and Prof. Nils-Goran Larsson (Karolinska Institutet) for sharing the
241 *tam^{KO}* mutant. This work is funded by NIH grant GM120005 to POF and Wellcome Trust grant
242 202269/Z/16/Z to HM.

243 **Author Contributions**

244 Conceptualization, A.C.Y.C., H.M. and P.H.O'F.; Investigation, A.C.Y.C., E.M., and H.M.;
245 Methodology, A.C.Y.C. and H.M.; Writing – Original Draft, P.H.O'F. and H.M.; Writing – Review
246 & Editing, P.H.O'F. and H.M.; Funding Acquisition, P.H.O'F. and H.M.; Supervision, P.H.O'F.
247 and H.M.

248 **Declaration of Interests**

249 We declare that there is no conflict of interest.

250 **Figure legends**

251

252 **Figure 1. A deficiency screen identified two overlapping deletion lines that significantly**
253 **increased the proportion of *mt:yak*.**

254 **A)** The stable heteroplasmic line: The *D. melanogaster* mtDNA (blue circle) has two
255 mutations, *ND2^{del1}* and *CoI^{T300I}*. *ND2^{del1}* is a 9 bp in-frame deletion in the gene encoding NADH-
256 dehydrogenase 2 (dark blue); it is a viable hypomorphic allele. *CoI^{T300I}* is a temperature
257 sensitive allele of cytochrome *c* oxidase I (dark blue); when homoplasmic, it is lethal at 29 °C
258 but viable at lower temperatures. While *mt:yak* (pink circle) is fully functional in *D. melanogaster*,
259 it does not usually compete successfully with the endogenous wild-type
260 *D. melanogaster* mtDNA. However, *mt:yak* is stably transmitted with *mt:ND2^{del1}+CoI^{T300I}* for over
261 70 generations at 29 °C[8]. **B)** The genetic cross scheme to introduce deletion chromosomes
262 (Table S1) into the stable heteroplasmic line (only shown for the 2nd chromosome deficiencies,
263 schematized by a bracketed interruption). First, 10 *Kr^f/CyO* heteroplasmic females (Generation
264 0) were crossed to 5 deficiency/*CyO* (Def/*CyO*) males to generate 10-20 female progeny with
265 the genotype of Def/*CyO* (generation 1), which were further crossed to 10 *Kr^f/CyO* males to
266 produce progeny (generation 2). Def/*CyO* males of generation 2 were collected to measure the
267 *mt:yak* percentage via qPCR. For some deficiencies, Def/*CyO* males were collected at multiple
268 generations to follow the *mt:yak* percentage over time. In controls, *Kr^f/CyO* males were used for
269 the first cross instead of Def/*CyO* males. All the subsequent steps were the same, and *Kr^f/CyO*
270 males of generation 2 were collected to measure the *mt:yak* percentage. **C)** Two overlapping
271 deficiencies (balanced by *CyO*) increased *mt:yak* transgenerationally (see also Table S2-S3).
272 The *mt:yak* percentage reached 100% after five generations (Error bars: standard deviation of
273 three independent experiments). **D)** The region deleted in both deficiencies contains 15 genes,
274 four of which encode mitochondrial proteins (red) (also refer to Figure S1).

275

276 **Figure 2. Reducing *tam* gene dose increased the abundance of functional mtDNA in two**
277 **heteroplasmic lines.**

278 **A)** Reducing the dose of *pol γ-β* or *GatC* showed no effect on mtDNA competition. On top, a
279 schematic shows the genomic arrangement of the co-transcribed genes *GatC* and *pol γ-β* (from
280 left to right) with the position and description of loss-of-function mutants isolated via
281 CRISPR/Cas9-based editing (Figure S2). The histogram below shows the *mt:yak* percentage for
282 different nuclear genotypes. Error bars: standard deviations of three independent experiments.
283 **B)** Heterozygosity for any of the three alleles of *tam* over the *CyO* chromosome dramatically
284 shifted the heteroplasmic ratio (see Figure S3 for the total mtDNA copy number of the *tam*
285 heterozygotes). On top, a schematic of Tam protein shows functional domains and the positions
286 of two homozygous lethal mutations *tam³* and *tam⁴*. At 29 °C, the *mt:yak* percentage increased
287 in *tam³*, *tam⁴* and *tam^{KO}* heterozygous mutants with a speed similar to that observed with the
288 BSC252 and BSC812 deficiencies (Figure 1C). Chromosomes bearing *tam* mutations were
289 introduced at generation 0 and the *mt:yak* percentage was followed over generations via qPCR
290 (solid line). From generation 1 to 3, only progeny heterozygous for the *tam* mutation were
291 followed and crossed to *Kr^f/CyO* to examine the cross-generational dose effect of *tam*. At
292 generation 4, the female progeny lacking the *tam* mutation were also mated with *Kr^f/CyO*, and
293 these populations were maintained in parallel for another 6 generations to assess the *mt:yak*
294 percentage (dotted lines). **C)** Reducing *tam* dose also increased the percentage of the
295 functional genome (*mt:ATP6[1]*) in the *mt:ATP6[1]/mt:ND2^{del1}+CoI^{T300I}* line. The percentage of
296 *mt:ATP6[1]* in two heteroplasmic lineages (control 1 and control 2) was measured over
297 generations at 29 °C. At generation 4, female progeny were divided into two populations: one
298 was mated with males heterozygous for *tam³* or *tam⁴* to remove one functional copy of *tam*, and
299 maintained in the heterozygous *tam* mutant background (balanced by *CyO*) for the subsequent

300 generations; the other population was mated with Kr^{fl}/CyO males as controls. All the controls
301 refer to Kr^{fl}/CyO .

302

303 **Figure 3. Reducing *tam* gene dosage enhances purifying selection.**

304 **A)** *tam* heterozygosity showed no effect on the dynamics of the *mt:yak* decline when the
305 *mt:yak/mt:ND2^{del1}+Col^{T300l}* line was cultivated at 22 °C, where the purifying selection against the
306 *mt:ND2^{del1}+Col^{T300l}* genome was significantly reduced. In both control and *tam* mutant
307 backgrounds (*tam³*, *tam⁴* or BSC252; balanced by *CyO*), the *mt:yak* was eliminated in two
308 generations. **B)** The decline of the *mt:Col^{T300l}* in the *mt:ND2^{del1}/mt:Col^{T300l}* line at the restrictive
309 temperature was accelerated in heterozygous *tam* mutants. The percentage of *mt:Col^{T300l}* was
310 followed in various flies with only one functional copy of *tam* (*tam³*, *tam^{KO}*, BSC252 or BSC812;
311 balanced by *CyO*) and Kr^{fl}/CyO nuclear background over generations. **C)** Reducing *tam* gene
312 dose enhanced the rate at which wild-type mtDNA overtook the *mt:ND2^{del1}* at 25 °C. The
313 percentage of the wild-type mtDNA was followed in various heterozygous *tam* mutants (*tam³*,
314 *tam^{KO}*, BSC252 or BSC812; balanced by *CyO*) and Kr^{fl}/CyO nuclear background. Error bars:
315 standard deviations of three or more independent experiments, *p*-value: Student's *t*-test. All the
316 controls refer to Kr^{fl}/CyO .

317

318 **Figure 4. Modulating Tam function alone is sufficient to influence competition between**
319 **mitochondrial genomes.**

320 **A)** The dose effect of *tam* on the percentage of *mt:yak* was not detected in nuclear backgrounds
321 where 2nd chromosomes unrelated to the *CyO* balancer were used. The *mt:yak* percentage was
322 followed in various heterozygous *tam* mutants (*tam³*, *tam^{KO}*, BSC252 or BSC812) balanced by
323 *CyO* related or unrelated 2nd chromosomes. A detailed cross scheme for each genotype is
324 presented in Figure S4D. **B)** Homozygous or transheterozygous viable *tam* mutants showed
325 that reducing functional Tam alone is sufficient to increase the percentage of *mt:yak* (see also
326 Figure S4). The top panel illustrates the cross scheme used to introduce various *tam* alleles into
327 the stable heteroplasmic line. The *mt:yak* percentage was followed in *tam^{Δ263D}/CyO*,
328 *tam^{Δ263D}/tam^{Δ263D}* and *tam^{Δ263D}/tam⁻* (*tam³* or *tam^{KO}*) adult males (see Figure S2 for the sequence
329 details of *tam^{Δ263D}*). **C)** Increasing *tam* dose decreased the percentage of *mt:yak*. The stable
330 heteroplasmy females were crossed to males homozygous for Tam-GFP on the 3rd chromosome
331 (BAC clone, a gift from Hong Xu, NIH) for two generations to produce heteroplasmic flies
332 containing two endogenous copies of *tam* on the 2nd chromosome and two extra copies of *tam*-
333 *GFP* on the 3rd chromosome. The *mt:yak* percentage was followed for four generations. Error
334 bars: standard deviations of three or more independent experiments, *p*-value: Student's *t*-test.

335 STAR Methods

336

337 Lead Contact and Materials Availability

338

339 Further information and requests for resources and reagents should be directed to and will be
340 fulfilled by the Lead Contact, Hansong Ma (hm555@cam.ac.uk). There are no restrictions to the
341 availability of reagents.

342

343 Experimental Model and Subject Details

344

345 The following flies were used in this study: Bloomington Deficiency Kits (Table S1), additional
346 deficiency lines that cover the entire *tam* gene (Df(2L)Exel7059 and Df(2L)FDD-0428643) or *twk*
347 gene (Df(2L)Exel7043) (BDSC:7826, BDSC:21566 and BDSC:7816, respectively), *tam*³ and
348 *tam*⁴ (BDSC:3410 and BDSC:25145), *tam*^{KO} (generated in [22]), BacTam (a gift from Hong Xu,
349 National Heart, Lung and Blood Institute), *nos-Cas9* (BDSC:54591) and four lines carrying the
350 *SM6a* balancer chromosome. All fly stocks were raised on standard media at 25 °C unless
351 otherwise stated.

352

353 Various heteroplasmic lines were generated via cytoplasmic transplantation as described in[5].
354 The stable *mt:yak/mt:ND2^{del1}+Col^{T3001}* was previously created by introducing cytoplasm of *D.*
355 *yakuba* into the *mt:ND2^{del1}+mt:Col^{T3001}* embryos[8]. After the stable heteroplasmy was
356 established, flies were balanced on the 2nd or 3rd chromosome by crossing to *Kr^{fl}/CyO* or
357 *MKRS/TM6B* males, respectively. Once balanced, the flies were continuously backcrossed to
358 *Kr^{fl}/CyO* or *MKRS/TM6B* males to maintain an isogenic nuclear background. To create
359 *mt:ATP6[1]/mt:ND2^{del1}+Col^{T3001}* line, cytoplasm of *mt:ND2^{del1}+Col^{T3001}* was injected into
360 *mt:ATP6[1]* embryos in order to create founder flies with a high percentage of *mt:ATP6[1]*. To
361 generate *mt:ND2^{del1}/mt:Col^{T3001}*, cytoplasm of *mt:ND2^{del1}* embryos was transferred to *mt:Col^{T3001}*
362 embryos to create heteroplasmic flies with a high percentage of *mt:Col^{T3001}*. To generate wild-
363 type/*mt:ND2^{del1}*, cytoplasm of wild-type embryos was transferred to *mt:ND2^{del1}* embryos to
364 create heteroplasmic flies with a high percentage of *mt:ND2^{del1}*. All the heteroplasmic lines were
365 maintained and examined at 29 °C, except the wild-type/*mt:ND2^{del1}* flies, which were maintained
366 at 25 °C instead.

367

368 Method Details

369

370 The deficiency screen cross scheme

371 The screen was carried out at 29 °C as shown in Figure 1B. Basically, for each deficiency, 5
372 males carrying the deletion chromosome were mated with 10 heteroplasmic females
373 (generation 0) balanced with either *Kr^{fl}/CyO* (for 2nd chromosome deficiencies) or *MKRS/TM6B*
374 (for 3rd chromosome deficiencies). After one generation, more than 10 female progeny
375 (generation 1) with an individual deletion chromosome balanced by *CyO* or *TM6B* were mated
376 with 10 *Kr^{fl}/CyO* or *MKRS/TM6B* males to maintain the deficiency and minimise variations in the
377 nuclear background. Total DNA from 10 to 40 young male progeny (generation 2) that carry the
378 deletion chromosome (balanced by *CyO* or *TM6B*) was extracted for qPCR analysis.
379 Heterozygous mutants of *tam*, *pol γ-β*, *GatC*, and *twk* were tested with the same experimental
380 setup for every generation. For controls, *Kr^{fl}/CyO* males were used instead of deficiency males
381 for the first cross.

382

383 CRISPR/Cas9-based mutagenesis

384 CRISPR/Cas9-based mutagenesis was performed as described on FlyCRISRP
385 (<https://flycrispr.org/>). In brief, two gRNAs were designed for each of the following genes: *pol γ-β*
386 (gaaaaacgctggatgtgac, gctttgatgttcagaagag), *GatC* (gcagctaacgcacccacca,
387 gatctggatttcggaggcgc), *twk* (tgctggcttacgtaaacaaag, atatctgggcatcgacggg), or *tam*
388 (gtcacaatgtctctacgac, ctacgacagggcgcgactga) using FlyCRISPR target finder
389 (<http://tools.flycrispr.molbio.wisc.edu/targetFinder/>). Complimentary oligos were synthesized by
390 Integrated DNA Technologies and were cloned into a pCFD5 plasmid. Plasmids were amplified
391 and purified, and then injected into *nos-Cas9* flies (BDSC:54591) at a concentration of 200 ng/μl.
392 Adults were then balanced by crossing to *Kr^{fl}/CyO* twice to establish individual stocks. The
393 mutated sequences were verified by Sanger sequencing.
394

395 **DNA extraction and quantitative PCR**

396 Total DNA extraction was performed as described in[5]. In brief, 10 to 40 adult males were
397 squashed in 500 μl of homogenization buffer (100 mM Tris-HCl (pH 8.8), 10 mM EDTA, 1%
398 SDS) and incubated at 70 °C for 30 min. Potassium acetate was added to a final concentration
399 of 1 M, and samples were incubated on ice for 30 min. Samples were centrifuged at 20,000 g
400 for 10 min at room temperature. DNA was recovered from the supernatant by adding 0.5x
401 volume of isopropanol followed by washing with 70% ethanol. DNA was then dissolved in 100 μl
402 Tris (10 mM, pH 8.0) before further dilution.
403

404 For all qPCR reactions, 2X SensiFast SYBR Green PCR Master Mix (Bioline 98020) was used
405 in 20 μl reactions with 500 nM of each primer. For each reaction, 5% of a male's total genomic
406 DNA was used as the template to allow the Ct values to land between cycles 10-25. Each qPCR
407 cycle was incubated at 95 °C for 10 min followed by 35 cycles of 95 °C for 30 s and 48 °C for 30
408 s. Standard curves were plotted using a series of tenfold dilutions (2×10^7 to 2×10^3 copies per
409 qPCR reaction) of the linearized PCR products containing regions covered by both the common
410 and specific primer sets. The efficiency of each primer set was normalized by comparison to
411 homoplasmic mtDNA that contain both the common and specific region. The absolute copy
412 number of targeted regions was calculated according to the Ct value and the standard curve for
413 one of the co-resident mtDNA genotypes (e.g. *mt:yak*, recognized by the specific primer set)
414 and total mtDNA (recognized by the common primer set). All the primers are listed in Table S4.
415

416 **Total RNA extraction and reverse transcription**

417 Total RNA from 2-day old males was extracted based on the TRIzol reagent (Invitrogen)
418 protocol. Ten males were ground with 750 μl of TRIzol reagent and incubated at room
419 temperature for 10 min. Phenol was removed from samples by multiple rounds of chloroform
420 extraction. RNA from the supernatant was precipitated by adding 0.5x isopropanol and washed
421 once with 70% ethanol. The extracted RNA was then treated with RNase-free DNase I (New
422 England Biolabs) for 30 min at 37 °C to remove genomic DNA. Subsequently, DNase activity
423 was heat-inactivated for 10 min at 65 °C upon adding 1 μl of 50 mM EDTA. The RNA was then
424 reverse-transcribed with Oligo (dT)₁₈ primer using RevertAid First-strand cDNA synthesis kit
425 (Invitrogen). The relative expression level of *tam* and *pol γ-β* was measured by qPCR and
426 normalized to the expression level of house-keeping gene *Act42A* or *EF1α*. For each qPCR
427 reaction, 2X SensiFast SYBR Green PCR Master mix (Bioline) was used in 20 μl reactions with
428 500 nM of each primer. The qPCR cycle was set as 95 °C for 10 min followed by 35 cycles of
429 95 °C for 30 s and elongation for 30 s. All the primers are listed in Table S4.
430

431 **Embryo mtDNA extraction and copy number measurement**

432 For each genotype, over 50 newly laid eggs (collected within 20 min after egg laying) were lysed
433 in 100 μl of QuickExtract buffer (Lucigen, Thermo Fisher Scientific) in Precellys homogenizer. In
434 brief, samples were agitated 3 times at 4,000 rpm for 30 s with a 30 s pause at room

435 temperature. The homogenised samples were then incubated for 15 min at 65 °C followed by 5
436 min at 95 °C. The total mtDNA copy number was then measured by qPCR using the common
437 primer set that binds to a conserved mtDNA region of *mt:yak* and *mt:ND2^{del1}+CoI^{T3001}* (Table S4).
438

439 **Quantification and Statistical Analysis**

440 As specified in all figure legends, the percentage of a given mitochondrial genotype in a
441 heteroplasmic line (Figure 1C, 2A, 3, 4A, 4B and S3C) was measured in at least three
442 independent biological replicates. Each replicate contained 10-40 young adult males. Similarly,
443 the total mtDNA copy number (Figure S3B) and the mRNA level of *tam* and *pol γ-β* genes
444 (Figure S3A and S4B) were measured in three independent biological replicates. For mtDNA
445 copy number quantifications, 50 newly laid eggs or ten 2-day old adult males were used for
446 each replicate. For mRNA level quantifications, each replicate included ten 2-day old adult
447 males. Figures are all presented as mean ± SD. All the statistical analyses were performed
448 using GraphPad Prism 7.0. Differences were examined by unpaired Student's *t*-test.
449 Significance was defined by $p < 0.05$ (*), $p < 0.005$ (**) and $p < 0.0005$ (***).
450

451 **Data and Code Availability**

452 This study did not generate datasets and codes.

453 **References**

454
455 1 Stewart JB, Freyer C, Elson JL, Wredenberg A, Cansu Z, Trifunovic A, Larsson NG. Strong
456 purifying selection in transmission of mammalian mitochondrial DNA. *PLoS Biol* 2008;6:e10–71.
457 2 Freyer C, Cree LM, Mourier A, Stewart JB, Koolmeister C, Milenkovic D, Wai T, Floros VI,
458 Hagstrom E, Chatzidaki EE, et al. Variation in germline mtDNA heteroplasmy is determined
459 prenatally but modified during subsequent transmission. *Nat Genet* 2012;44:1282–5.
460 3 Fan W, Waymire KG, Narula N, Li P, Rocher C, Coskun PE, Vannan MA, Narula J, Macgregor
461 GR, Wallace DC. A mouse model of mitochondrial disease reveals germline selection against
462 severe mtDNA mutations. *Science* 2008;319:958–62.
463 4 Floros VI, Pyle A, Dietmann S, Wei W, Tang WCW, Irie N, Payne B, Capalbo A, Noli L, Coxhead
464 J, et al. Segregation of mitochondrial DNA heteroplasmy through a developmental genetic
465 bottleneck in human embryos. *Nat Cell Biol* 2018;20:144–51.
466 5 Ma H, Xu H, O'Farrell PH. Transmission of mitochondrial mutations and action of purifying
467 selection in *Drosophila melanogaster*. *Nat Genet* 2014;46:393–7.
468 6 Hill JH, Chen Z, Xu H. Selective propagation of functional mitochondrial DNA during oogenesis
469 restricts the transmission of a deleterious mitochondrial variant. *Nat Genet* 2014;46:389–92.
470 7 Lieber T, Jeedigunta SP, Palozzi JM, Lehmann R, Hurd TR. Mitochondrial fragmentation drives
471 selective removal of deleterious mtDNA in the germline. *Nature* 2019;570:380–4.
472 8 Ma H, O'Farrell PH. Selfish drive can trump function when animal mitochondrial genomes
473 compete. *Nat Genet* 2016;48:798–802.
474 9 Tsang WY, Lemire BD. Stable heteroplasmy but differential inheritance of a large mitochondrial
475 DNA deletion in nematodes. *Biochem Cell Biol* 2002;80:645–54.
476 10 Volz-Lingenhöhl A, Solignac M, Sperlich D. Stable heteroplasmy for a large-scale deletion in the
477 coding region of *Drosophila subobscura* mitochondrial DNA. *Proc Natl Acad Sci USA*
478 1992;89:11528–32.
479 11 Clark KA, Howe DK, Gafner K, Kusuma D, Ping S, Estes S, Denver DR. Selfish Little Circles:
480 Transmission Bias and Evolution of Large Deletion-Bearing Mitochondrial DNA in
481 *Caenorhabditis briggsae* Nematodes. *PLoS ONE* 2012;7(7):e41433.
482 12 Phillips WS, Coleman-Hulbert AL, Weiss ES, Howe DK, Ping S, Wernick RI, Estes S, Denver DR.
483 Selfish Mitochondrial DNA Proliferates and Diversifies in Small, but not Large, Experimental
484 Populations of *Caenorhabditis briggsae*. *Genome Biol Evol* 2015;7:2023–37.
485 13 Kang E, Wu J, Gutierrez NM, Koski A, Tippner-Hedges R, Agaronyan K, Platero-Luengo A,
486 Martinez-Redondo P, Ma H, Lee Y, et al. Mitochondrial replacement in human oocytes carrying
487 pathogenic mitochondrial DNA mutations. *Nature* 2016;540:270–5.
488 14 Battersby BJ, Loredó-Osti JC, Shourbridge EA. Nuclear genetic control of mitochondrial DNA
489 segregation. *Nat Genet* 2003;33:183–6.
490 15 Matsuura ET, Tanaka YT, Yamamoto N. Effects of the nuclear genome on selective
491 transmission of mitochondrial DNA in *Drosophila*. *Genes Genet Syst* 1997;72:119–23.
492 16 Farge G, Touraille S, Le Goff S, Petit N, Renoux M, Morel F, Alziari S. The nuclear genome is
493 involved in heteroplasmy control in a mitochondrial mutant strain of *Drosophila subobscura*. *Eur*
494 *J Biochem* 2002;269:998–1005.
495 17 Jenuth JP, Peterson AC, Shourbridge EA. Tissue-specific selection for different mtDNA
496 genotypes in heteroplasmic mice. *Nat Genet* 1997;16:93–5.
497 18 Jokinen R, Marttinen P, Sandell HK, Manninen T, Teerenhovi H, Wai T, Teoli D, Loredó-Osti JC,
498 Shourbridge EA, Battersby BJ. Gimap3 Regulates Tissue-Specific Mitochondrial DNA
499 Segregation. *PLoS Genet* 2010;6(10):e1001161.
500 19 Roote J, Russell S. Toward a complete *Drosophila* deficiency kit. *Genome Biol* 2012;13:149.
501 20 Cook RK, Christensen SJ, Deal JA, Coburn RA, Deal ME, Gresens JM, Kaufman TC, Cook KR.
502 The generation of chromosomal deletions to provide extensive coverage and subdivision of the
503 *Drosophila melanogaster* genome. *Genome Biol* 2012;13:R21.
504 21 Iyengar B, Roote J, Campos AR. The *tamas* gene, identified as a mutation that disrupts larval
505 behavior in *Drosophila melanogaster*, codes for the mitochondrial DNA polymerase catalytic
506 subunit (DNApol-gamma125). *Genetics* 1999;153:1809–24.

507 22 Bratic A, Kauppila TES, Macao B, Groenke S, Siibak T, Stewart JB, Baggio F, Dols J, Partridge
508 L, Falkenberg M, et al. Complementation between polymerase- and exonuclease-deficient
509 mitochondrial DNA polymerase mutants in genomically engineered flies. *Nat Commun*
510 2015;6:8808

511 23 Ma H, O'Farrell PH. Selections that isolate recombinant mitochondrial genomes in animals. *Elife*
512 2015;4:e07247. doi:10.7554/eLife.07247.

513 24 Zhang Y, Wang Z-H, Liu Y, Chen Y, Sun N, Gucek M, Zhang F, Xu H. PINK1 Inhibits Local
514 Protein Synthesis to Limit Transmission of Deleterious Mitochondrial DNA Mutations. *Mol Cell*
515 2019; 73(6):1127-37

516 25 Yu Z, O'Farrell PH, Yakubovich N, DeLuca SZ. The Mitochondrial DNA Polymerase Promotes
517 Elimination of Paternal Mitochondrial Genomes. *Curr Biol* 2017;27:1033–9.

518 26 Peeva V, Blei D, Trombly G, Corsi S, Szukszto MJ, Rebelo-Guiomar P, Gammage PA, Kudin AP,
519 Becker C, Altmuller J, et al. Linear mitochondrial DNA is rapidly degraded by components of the
520 replication machinery. *Nat Commun* 2018;9(1):1727.

521 27 Nissanka N, Bacman SR, Plastini MJ, Moraes CT. The mitochondrial DNA polymerase gamma
522 degrades linear DNA fragments precluding the formation of deletions. *Nat Commun* 2018;9:2491.

523 28 Chan SSL, Copeland WC. DNA polymerase gamma and mitochondrial disease: understanding
524 the consequence of POLG mutations. *Biochim Biophys Acta* 2009;1787:312–9..

TABLE FOR AUTHOR TO COMPLETE

Please upload the completed table as a separate document. **Please do not add subheadings to the Key Resources Table.** If you wish to make an entry that does not fall into one of the subheadings below, please contact your handling editor. (NOTE: For authors publishing in Current Biology, please note that references within the KRT should be in numbered style, rather than Harvard.)

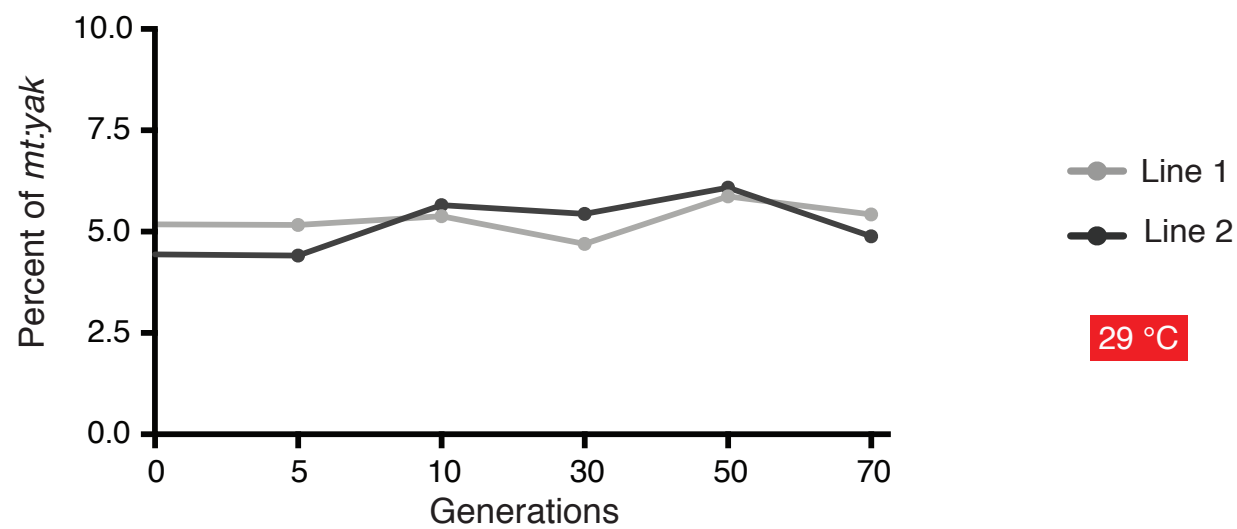
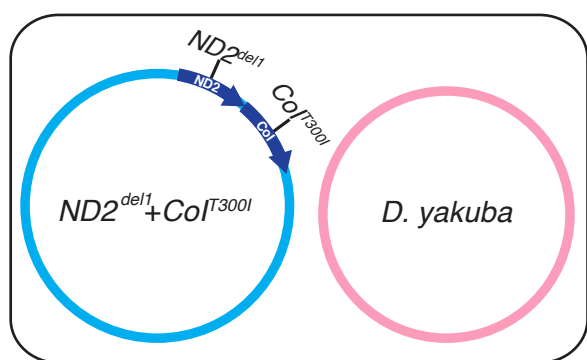
KEY RESOURCES TABLE

REAGENT or RESOURCE	SOURCE	IDENTIFIER
Antibodies		
Bacterial and Virus Strains		
Biological Samples		
Chemicals, Peptides, and Recombinant Proteins		
Critical Commercial Assays		
Deposited Data		
Experimental Models: Cell Lines		
Experimental Models: Organisms/Strains		
<i>D. melanogaster</i> : Bloomington Deficiency Kit	Bloomington Drosophila Stock Center	https://bdsc.indiana.edu/stocks/df/dfkit.html
<i>D. melanogaster</i> : <i>twk</i> mutants (<i>twk</i> ¹ and <i>twk</i> ²), <i>GatC</i> mutants (<i>GatC</i> ¹ and <i>GatC</i> ²), <i>tam</i> mutants (<i>tam</i> ^{A262Y} and <i>tam</i> ^{A263D}), <i>pol</i> γ - β mutants (<i>pol</i> γ - β ¹ and <i>pol</i> γ - β ²), see Figure S2	This paper	N/A

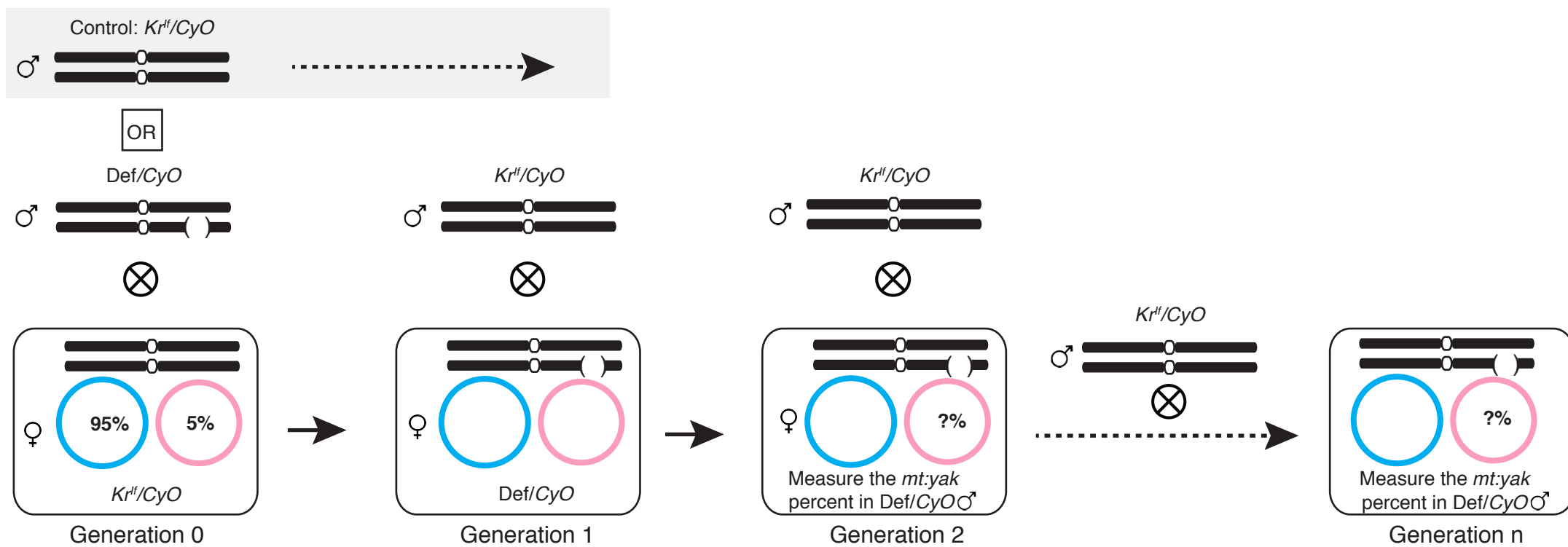
<i>D. melanogaster: tam</i> ^{KO}	[22]	DOI: 10.1038/ncomms9808 (2015)
<i>D. melanogaster: BacTam-GFP</i>	Hong Xu (NIH)	N/A
<i>D. melanogaster: tam</i> ³	Bloomington Drosophila Stock Center	BDSC:3410
<i>D. melanogaster: tam</i> ⁴	Bloomington Drosophila Stock Center	BDSC:25145
<i>D. melanogaster: Df(2L)Exel7059,</i>	Bloomington Drosophila Stock Center	BDSC:7826
<i>D. melanogaster: Df(2L)FDD-0428643</i>	Bloomington Drosophila Stock Center	BDSC:25166
<i>D. melanogaster: Df(2L)Exel7043</i>	Bloomington Drosophila Stock Center	BDSC:7816
<i>D. melanogaster: nos-Cas9</i>	Bloomington Drosophila Stock Center	BDSC:54591
Oligonucleotides		
Primers for qPCR, see Table S4	This paper	N/A
Primers for RT-qPCR, see table S4	This paper	N/A
Recombinant DNA		
pCDF5+guide RNA for CRISPR/Cas9-based editing for the following genes (<i>twk</i> , <i>GatC</i> , <i>tam</i> and <i>pol γ-β</i>)	This paper	N/A
Software and Algorithms		
Guide RNA design for the following genes (<i>twk</i> , <i>GatC</i> , <i>tam</i> and <i>pol γ-β</i>)	FLYCRISPR	https://flycrispr.org/
Other		
Sequence data of <i>tam</i> ROF of a number of 2 nd chromosomes (<i>D. melanogaster</i>), See Figure S4A	This paper	N/A

Figure 1

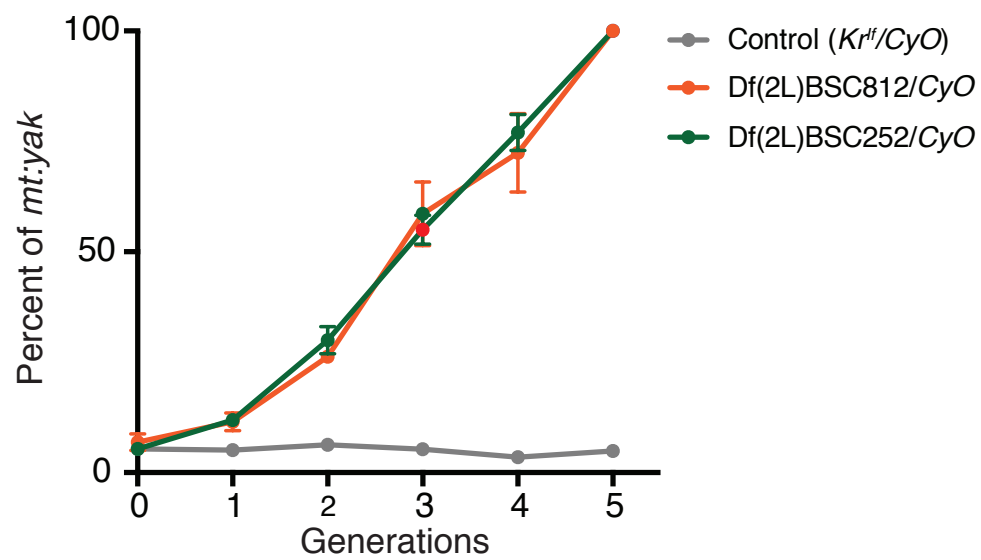
A



B



C



D

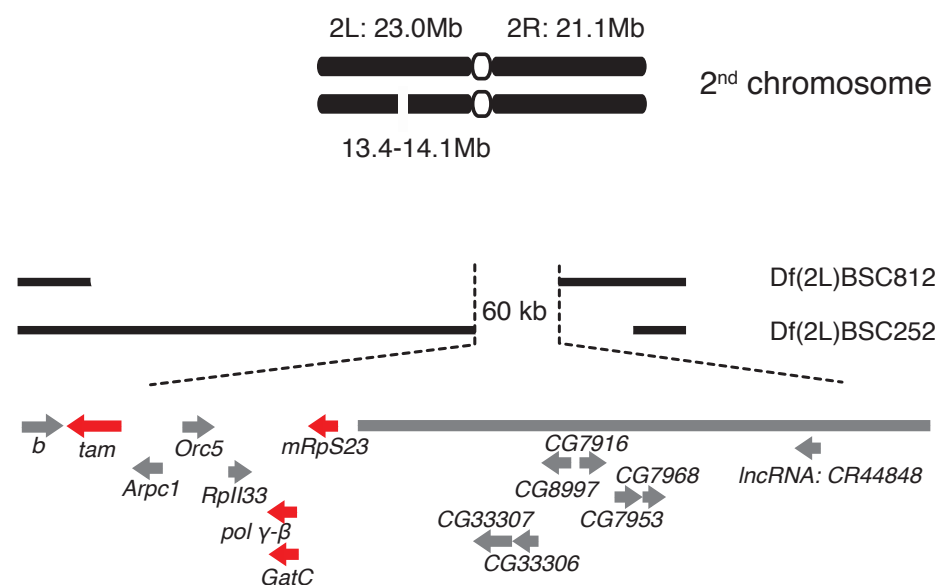


Figure 2

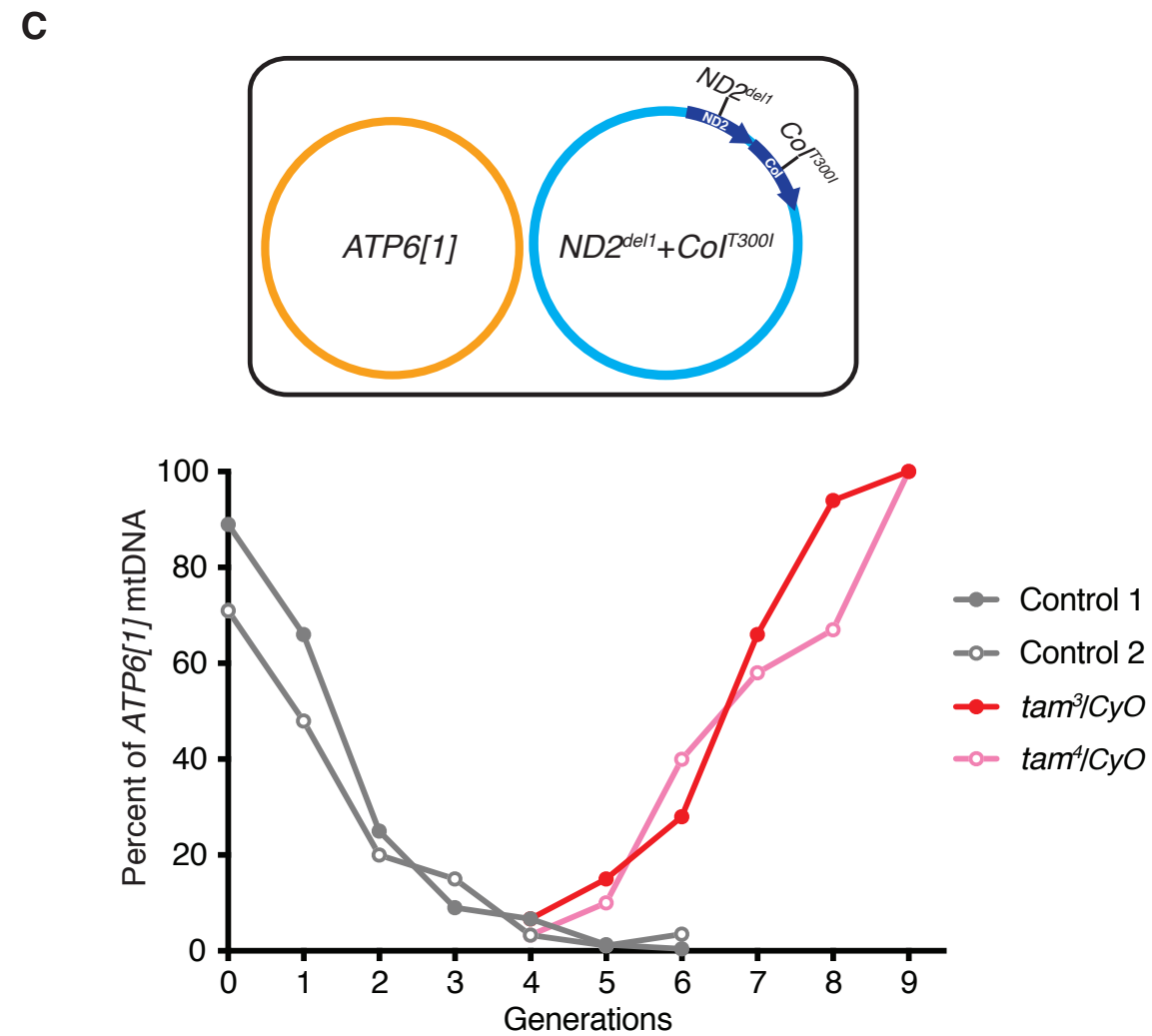
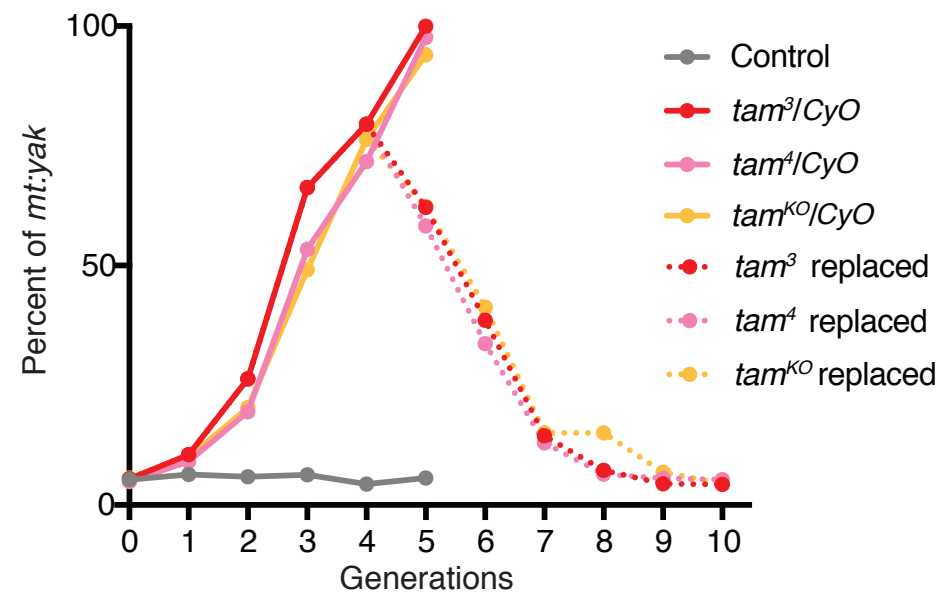
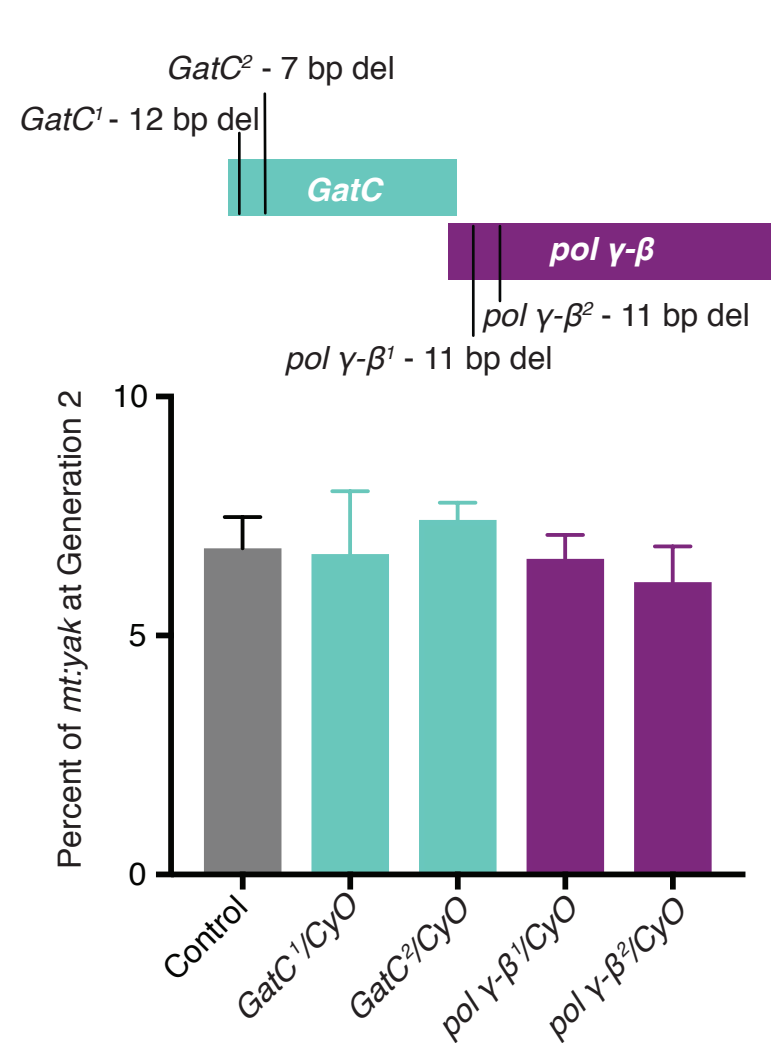


Figure 3

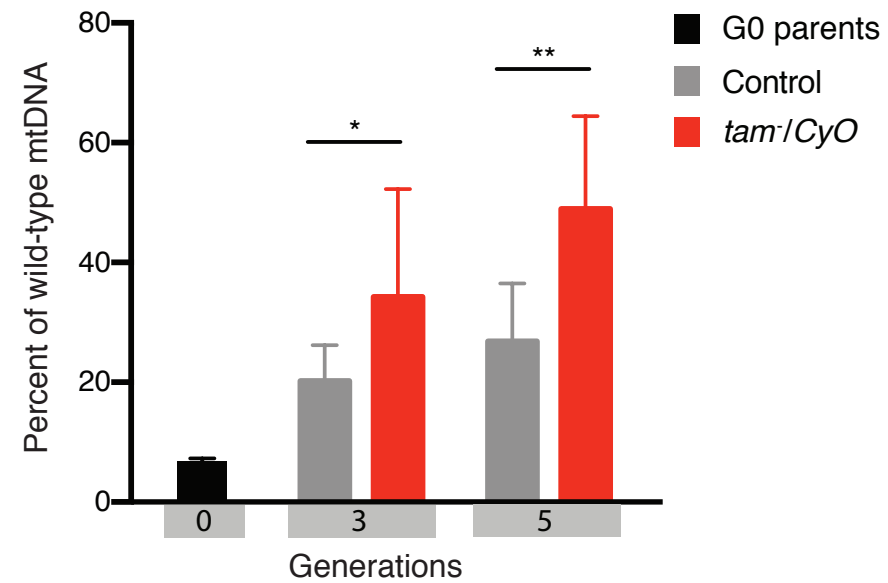
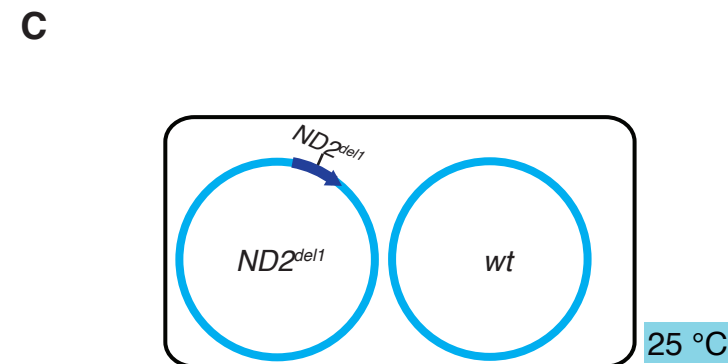
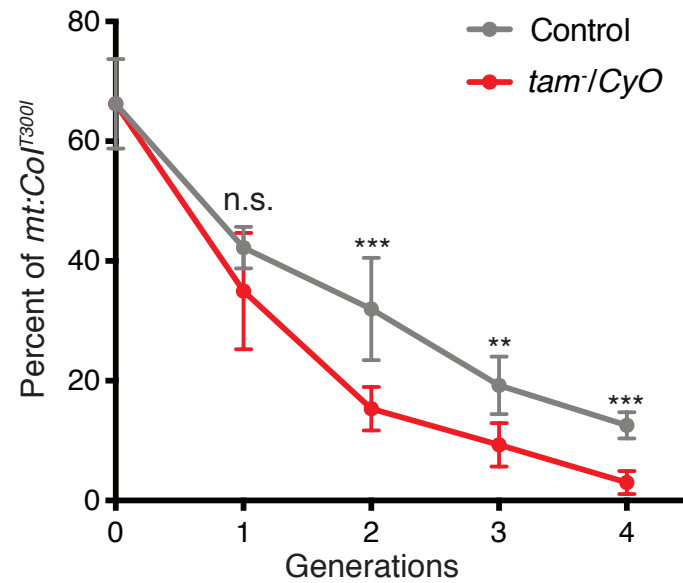
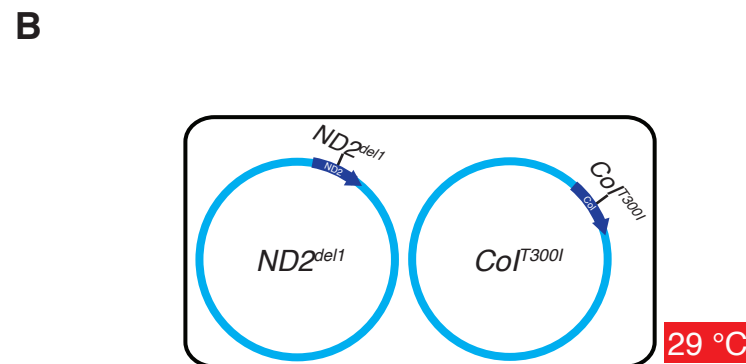
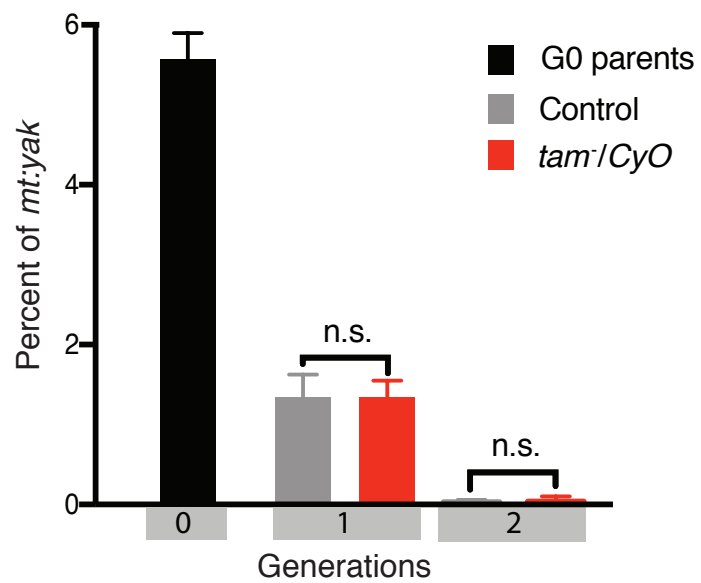
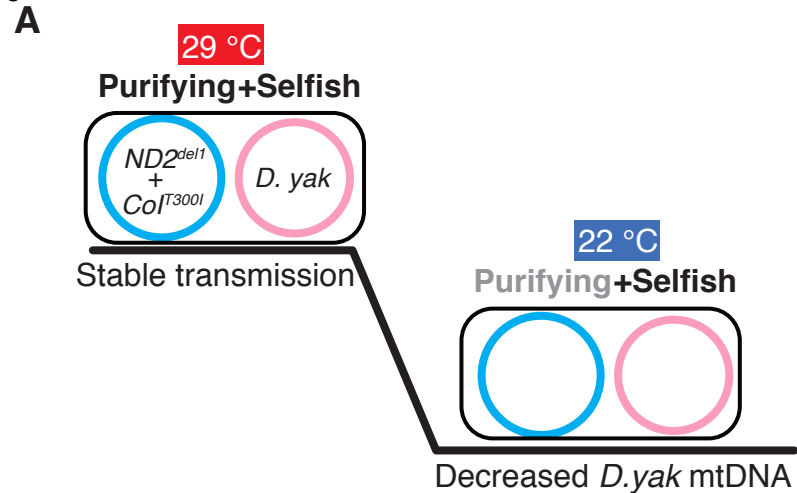
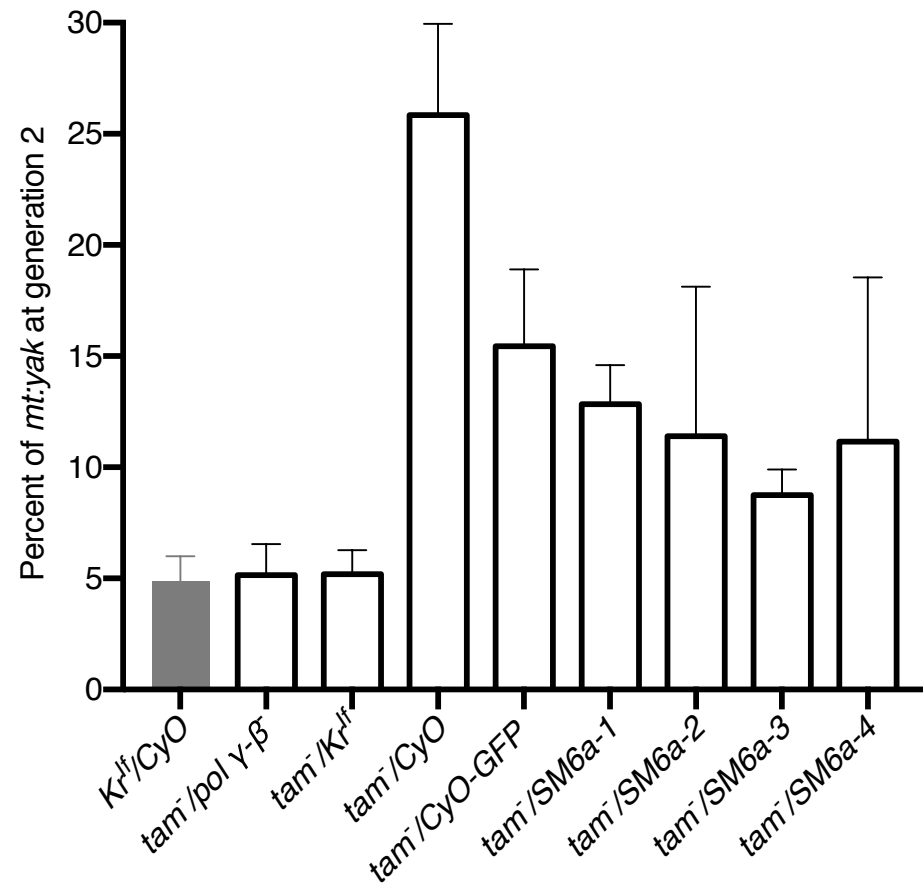
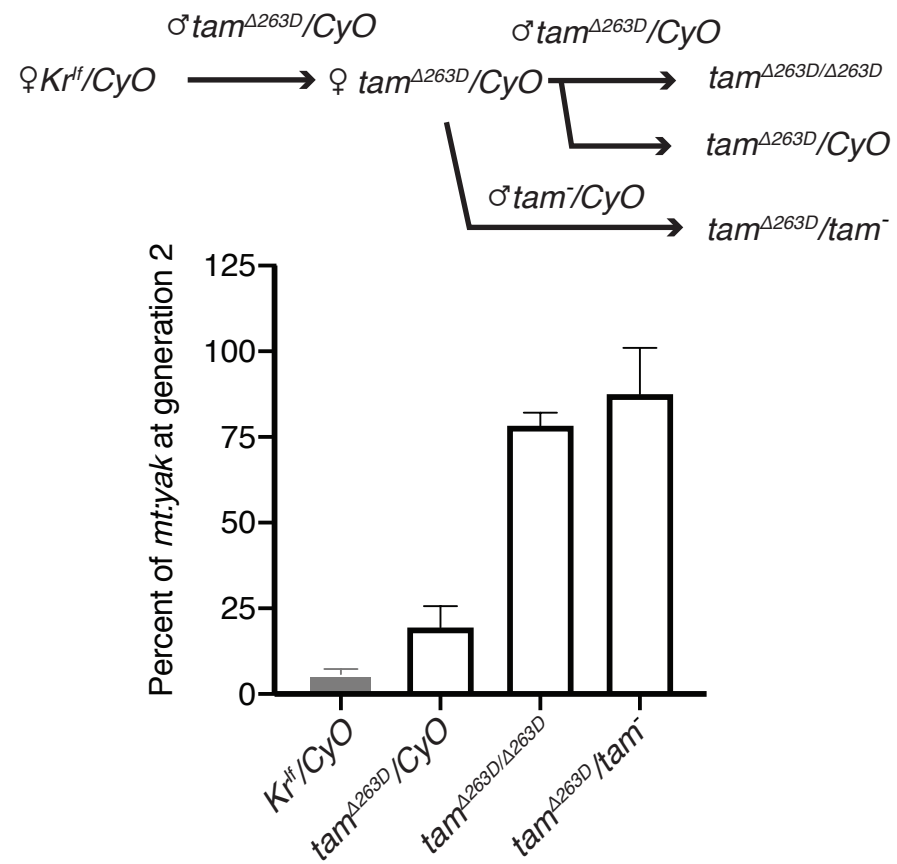


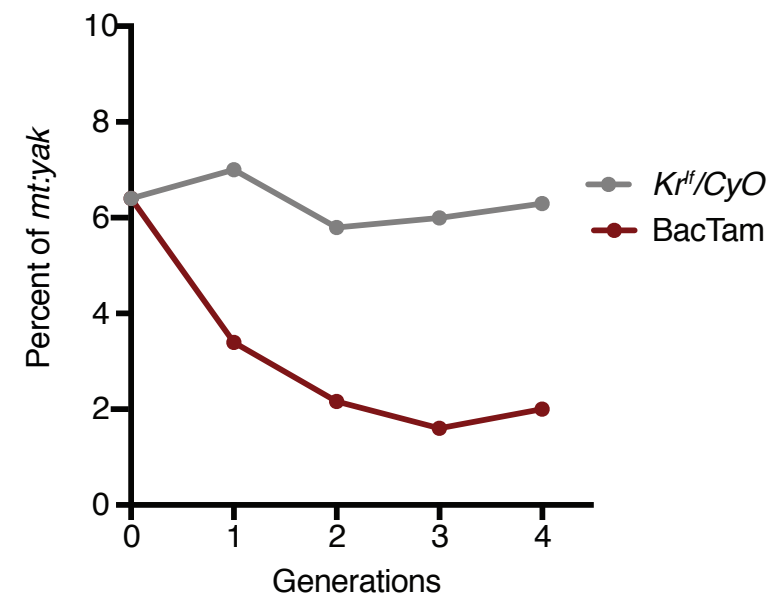
Figure 4
A



B



C



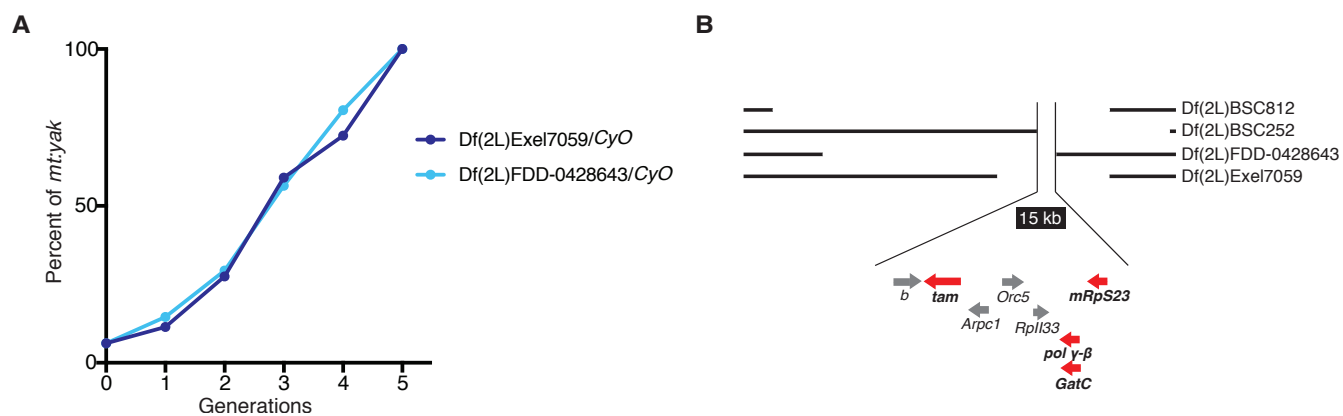


Figure S1. Two additional deficiencies that cover the *tam* genomic region showed an increased *mt:yak* percentage over generations. Related to Figure 1.

A) In Df(2L)Exel7059 and Df(2L)FDD-0428643 lines, the *mt:yak* took over after five generations. **B)** The common region deleted by the four deficiencies that similarly modified the heteroplasmy dynamic is indicated. It is 15 kb in size and contains eight genes, four of which encode mitochondrial proteins (red).

GatC 28 **Q L T H P T K V P Q T**
 CAGCTAACGCATCCCACCAAGGTGCCACAGACA
GatC¹ **Q P K V P Q T**
 CAGC-----CCAAGGTGCCACAGACA

GatC 47 **T S A S E I Q I D T K L**
 ACCAGCGCCTCCGAAATCCAGATCGACACGAAA...CTAA
GatC² **T P K S R S T R K** *⁷⁷
 A-----CTCCGAAATCCAGATCGACACGAAA...CTAA

pol γ-β 62 **V N I Q R F S F P Q S Q Q F R N**
 GTCAACATCCAGCGTTTTTCTTTCCACAAAGCCAGCAATTCCGTAAC
pol γ-β¹ **A F F L S T K P A I P** *⁷³
 G-----CGTTTTTCTTTCCACAAAGCCAGCAATTCCGTTAAAC

pol γ-β 94 **T L L K H Q S T C S G P T S**
 ACTCTTCTGAAACATCAAAGCACTTGTCTGGTCCCCTAGC
pol γ-β² **T S K H L F W S H** *¹⁰³
 AC-----ATCAAAGCACTTGTCTGGTCCCCTAGC

twk 88 **G L L A Y V N K R T G A F K**
 GGGCTGCTGGCTTACGTAAACAAGCGGACGGGAGCCTTT...TAAG
twk¹ **G L L A Y G S L Y** *¹²¹
 GGGCTGCTGGCTTACG-----GGAGCCTTTAT...TAA
twk² **G L I R E P L** *¹⁰¹
 GGGTCG-----ATACGGGAGCCTTT...TAA

tam 254 **L V V G H N V S Y D R A R L K**
 CTGGTGGTGGGTCACAATGTCTCCTACGACAGGGCGCGACTGAAG
tam^{Δ262Y} **L V V G H N V S D R A R L K**
 CTGGTGGTGGGTCACAATGTCTCC-----GACAGGGCGCGACTGAAG
tam^{Δ263D} **L V V G H N V S Y R A R L K**
 CTGGTGGTGGGTCACAATGTCTCTAC-----AGGGCGCGACTGAAG

Figure S2. Sequence details of *GatC*, *pol γ-β*, *twk* and *tam* mutants generated by CRISPR/Cas9-based editing. Related to Figures 2, 4, S3 and S4.

Wild-type DNA and amino acid sequences (bold) are displayed in parallel to the mutant sequences with deletions (hyphen lines) that lead to frameshift changes in amino acid sequence (red) and a stop codon at the position indicated (asterisk, number of amino acid residues incorporated). The lethal phase of homozygote *twk* and *pol γ-β* mutants was in early pupation, whereas homozygous *GatC* mutants only reach late embryonic or early 1st instar larval stages. The *GatC* mutants were trans-heterozygous viable when crossed to the two *pol γ-β* mutants, indicating that the isolated mutants affected the targeted gene without inactivating its co-transcribed partner. Each *tam* mutant carries a 3 bp deletion, which removes a single amino acid at the highly conserved exonuclease domain. Both are homozygous viable but female sterile. For the amino acid residue 263, a D to A mutation has been previously reported to increase mtDNA mutation load over generations in *Drosophila* [S1, S2].

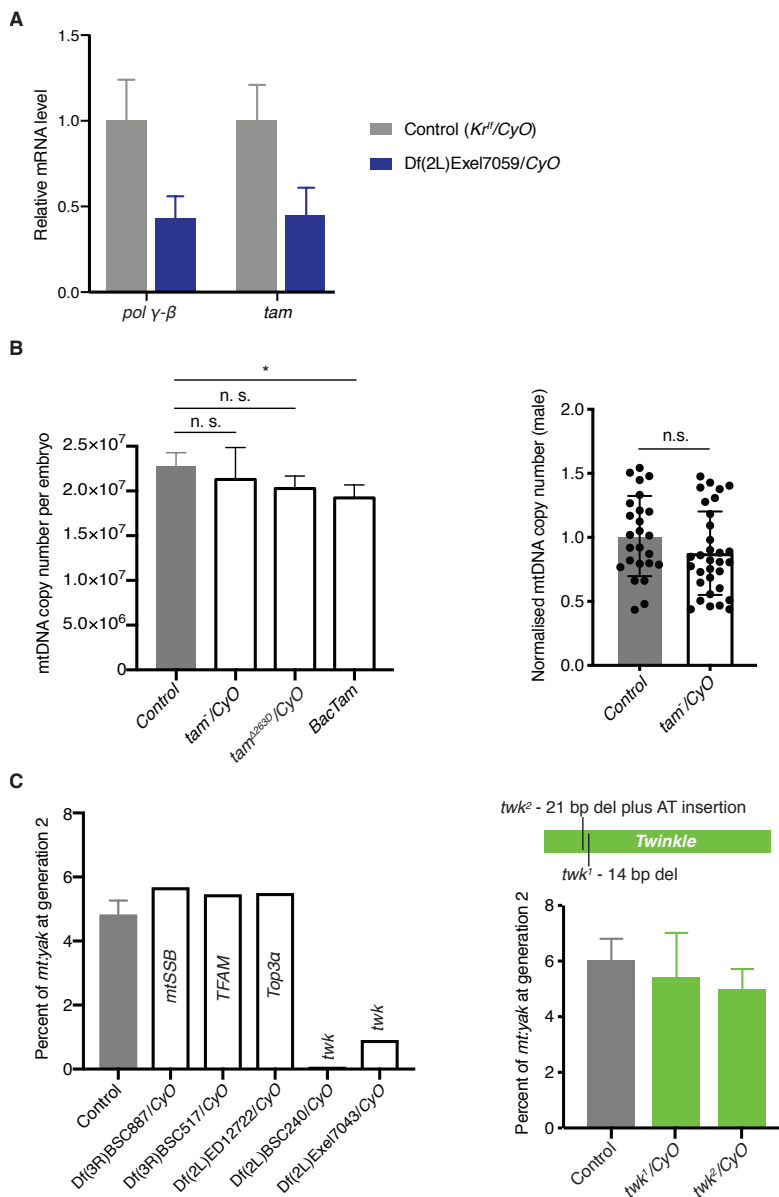
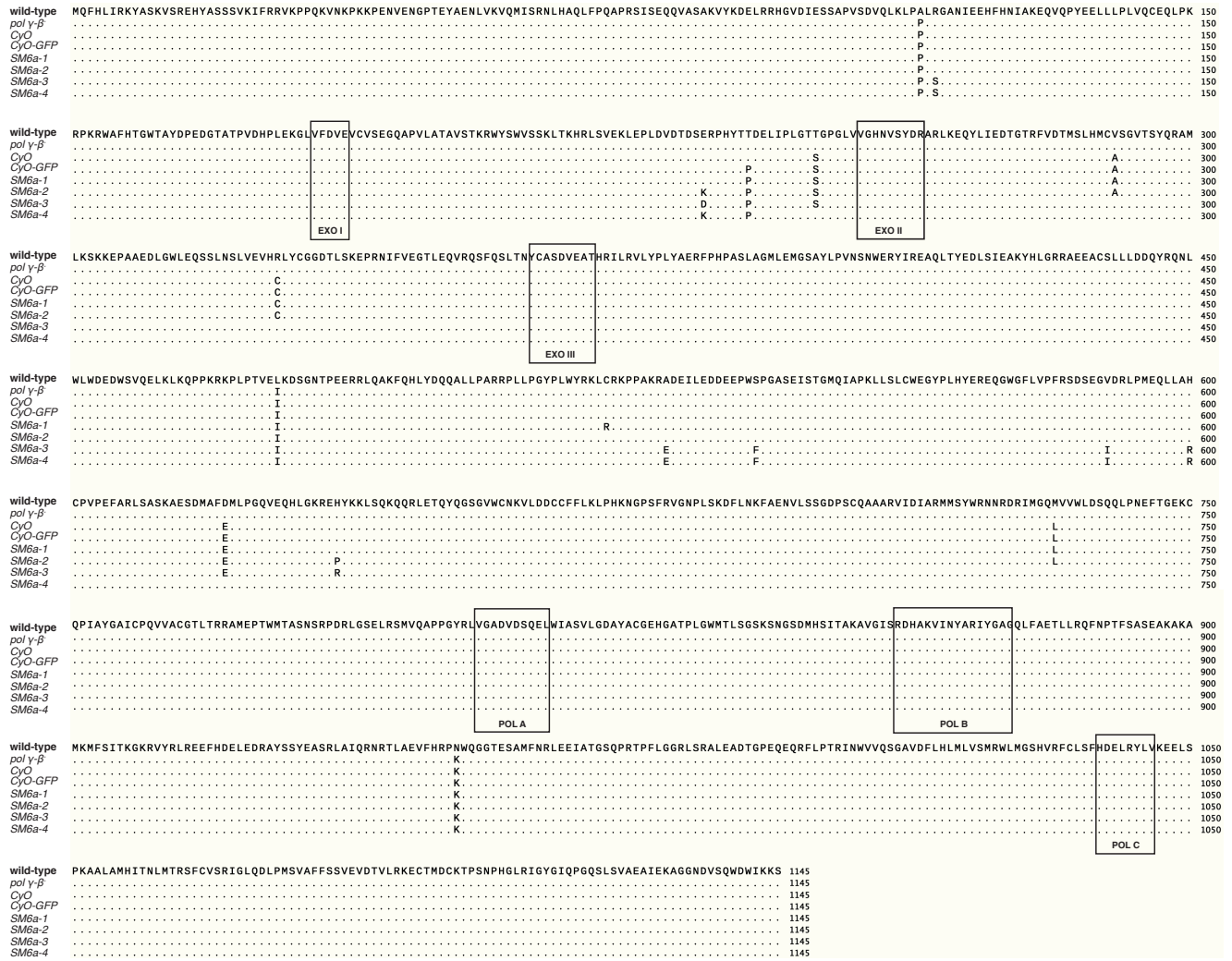


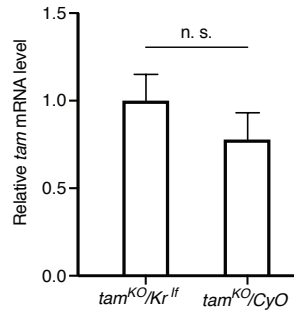
Figure S3. Characterisation of different deficiencies and heterozygous mutants to assess the impact of replication proteins on the total mtDNA copy number and mtDNA competition. Related to Figure 2.

A) The relative mRNA levels of *tam* and *pol γ-β* in adult male of *Df(2L)Exel7059* were about half compared to those of *Kr^{fl}/CyO*. Each sample represents an independent RNA extraction from a group of ten 2-day old adult males ($n=3$, Student's *t*-test, error bars: SD). **B)** The heterozygous *tam* mutants (*tam³*, *tam⁴*, *tam^{KO}* and *tam^{A263D}*) have a similar total mtDNA copy number compared to *Kr^{fl}/CyO* flies. Left panel: the absolute mtDNA copy number per egg was measured in newly laid eggs by qPCR ($n=3$, *p*-value: Student's *t*-test, error bars: SD). Each sample represents an extraction from a group of more than 50 eggs. Right panel: The mtDNA copy number per adult male was measured by qPCR and then normalized to the input amount of DNA. Each sample represents an extraction from a group of ten 2-day old adult males ($n>25$, *p*-value: Student's *t*-test, error bars: SD). **C)** Other components of mtDNA replication machinery show no dosage-dependent impact on mtDNA competition. Left panel: the abundance of *mt:yak* was not changed in deficiency lines that delete one genomic copy of *mtSSB*, *TFAM* or *Top3α*, but was reduced in deficiencies removing one copy of *twk*. Right panel: heterozygous *twk* mutants showed no change in the *mt:yak* percentage in two generations. The two *twk* mutants were isolated by CRISPR/Cas9-based editing (Figure S2, error bars: SD).

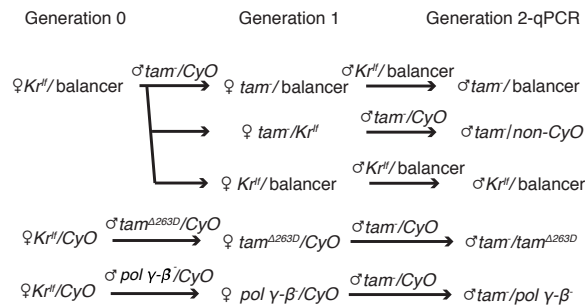
A



B



D



C

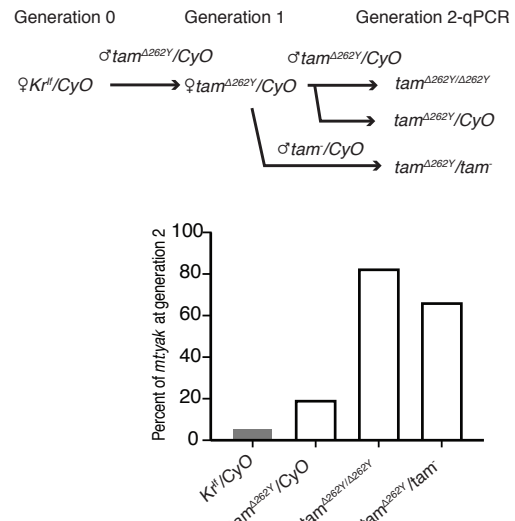


Figure S4. Modulating Tam function alone is sufficient to influence competition between mitochondrial genomes. Related to Figure 4.

A) The *tam* sequence for *CyO* related or unrelated 2nd chromosomes. The detailed lineages of the *CyO* related chromosomes are uncertain and the sequences appear to be at odds with a shared heritage among *SM6a* chromosomes. Flies carrying *SM6a-2*, *SM6a-3* and *SM6a-4* were obtained from the Bloomington *Drosophila* Stock Centre, and their stock numbers are 25166, 8045 and 27383, respectively. The amino acids that do not differ from the wild-type allele are indicated by dots. The three conserved exonuclease and polymerase domains are labelled (refer to [S3]). **B)** The relative mRNA level of *tam* in *tam*^{KO} heterozygous with *Kr^{lf}* or *CyO* balancer chromosomes. Each sample represents an independent RNA extraction from a group of ten 2-day old adult males (n=3, Student's *t*-test, error bars: SD). **C)** Homozygous or transheterozygous viable *tam* mutants revealed that reducing functional Tam alone is sufficient to increase the *mt:yak* percentage. The top panel illustrates the cross scheme used to introduce various *tam* alleles into the stable heteroplasmic line. The *mt:yak* percentage was measured in *tam*^{Δ262Y}/*CyO*, *tam*^{Δ262Y}/*tam*^{Δ262Y} and *tam*^{Δ262Y}/*tam* (*tam*^{KO}) adult males. **D)** The cross scheme to generate *tam* heterozygotes with *CyO* related or unrelated 2nd chromosomes used in Figure 4A.

Table S1. A list of all deficiencies tested in this study. Related to Figure 1.

<u>Df(2L)al</u>	Df(2L)ED441	Df(2R)BSC702	<u>Df(3L)BSC419</u>	Df(3R)BSC633
Df(2L)ast2	<u>Df(2L)ED4651</u>	Df(2R)BSC769	Df(3L)BSC449	<u>Df(3R)BSC650</u>
Df(2L)BSC106	<u>Df(2L)ED489</u>	Df(2R)BSC780	Df(3L)BSC671	Df(3R)BSC677
Df(2L)BSC107	Df(2L)ED50001	Df(2R)BSC782	Df(3L)BSC673	<u>Df(3R)BSC681</u>
Df(2L)BSC109	Df(2L)ED5878	Df(2R)BSC784	Df(3L)BSC730	Df(3R)BSC728
Df(2L)BSC110	Df(2L)ED629	<u>Df(2R)BSC787</u>	<u>Df(3L)BSC774</u>	Df(3R)BSC738
Df(2L)BSC111	Df(2L)ED678	Df(2R)BSC821	<u>Df(3L)BSC775</u>	<u>Df(3R)BSC741</u>
<u>Df(2L)BSC142</u>	<u>Df(2L)ED690</u>	<u>Df(2R)BSC865</u>	Df(3L)BSC797	Df(3R)BSC748
Df(2L)BSC143	Df(2L)ED761	Df(2R)BSC880	Df(3L)BSC800	Df(3R)BSC749
Df(2L)BSC145	Df(2L)ED775	Df(2R)BSC883	Df(3L)BSC815	Df(3R)BSC750
Df(2L)BSC148	Df(2L)ED7853	Df(2R)BSC885	Df(3L)BSC816	Df(3R)BSC790
Df(2L)BSC149	Df(2L)ED793	Df(2R)BSC889	Df(3L)BSC845	Df(3R)BSC793
Df(2L)BSC151	Df(2L)ED8142	<u>Df(2R)CX1</u>	Df(3L)BSC884	Df(3R)BSC819
Df(2L)BSC159	Df(2L)ED94	<u>Df(2R)ED1612</u>	Df(3L)ED201	Df(3R)BSC874
Df(2L)BSC165	Df(2L)Exel6005	Df(2R)ED1673	Df(3L)ED208	Df(3R)BSC887
Df(2L)BSC169	Df(2L)Exel6009	Df(2R)ED1715	Df(3L)ED210	<u>Df(3R)ED10639</u>
<u>Df(2L)BSC17</u>	Df(2L)Exel6011	Df(2R)ED1725	Df(3L)ED217	Df(3R)ED10642
Df(2L)BSC172	Df(2L)Exel6012	Df(2R)ED1742	Df(3L)ED229	Df(3R)ED10845
Df(2L)BSC180	Df(2L)Exel6038	<u>Df(2R)ED1770</u>	Df(3L)ED230	<u>Df(3R)ED2</u>
Df(2L)BSC188	Df(2L)Exel6277	Df(2R)ED1791	<u>Df(3L)ED4196</u>	<u>Df(3R)ED50003</u>
Df(2L)BSC204	<u>Df(2L)Exel7011</u>	Df(2R)ED2219	Df(3L)ED4287	Df(3R)ED5100
Df(2L)BSC208	Df(2L)Exel7034	Df(2R)ED2247	Df(3L)ED4293	Df(3R)ED5147
Df(2L)BSC209	Df(2L)Exel7070	Df(2R)ED2354	Df(3L)ED4341	Df(3R)ED5156
Df(2L)BSC213	<u>Df(2L)Exel8038</u>	Df(2R)ED2426	Df(3L)ED4421	Df(3R)ED5177
Df(2L)BSC214	<u>Df(2L)J39</u>	Df(2R)ED2457	Df(3L)ED4457	<u>Df(3R)ED5330</u>
Df(2L)BSC227	Df(2L)It109	Df(2R)ED2487	Df(3L)ED4470	Df(3R)ED5339
<u>Df(2L)BSC233</u>	<u>Df(2L)M24F-B</u>	Df(2R)ED2747	Df(3L)ED4475	Df(3R)ED5428
Df(2L)BSC240	<u>Df(2L)r10</u>	Df(2R)ED3385	<u>Df(3L)ED4486</u>	Df(3R)ED5474
Df(2L)BSC241	<u>Df(2L)tkv3</u>	Df(2R)ED3610	Df(3L)ED4502	<u>Df(3R)ED5514</u>
Df(2L)BSC244	Df(2R)14H10W-35	Df(2R)ED3683	Df(3L)ED4543	Df(3R)ED5577
Df(2L)BSC252	Df(2R)BSC132	Df(2R)ED3728	Df(3L)ED4674	<u>Df(3R)ED5578</u>
Df(2L)BSC256	Df(2R)BSC135	Df(2R)ED3791	Df(3L)ED4710	<u>Df(3R)ED5623</u>
Df(2L)BSC277	Df(2R)BSC152	Df(2R)ED50004	<u>Df(3L)ED4858</u>	Df(3R)ED5644
Df(2L)BSC278	Df(2R)BSC161	Df(2R)Exel6061	Df(3L)ED4978	<u>Df(3R)ED5705</u>
<u>Df(2L)BSC291</u>	Df(2R)BSC19	Df(2R)Exel6062	Df(3L)ED50002	Df(3R)ED5718
Df(2L)BSC292	Df(2R)BSC199	Df(2R)Exel6064	Df(3L)ED5017	Df(3R)ED5780
Df(2L)BSC295	Df(2R)BSC267	Df(2R)Exel6066	Df(3L)Exel6085	Df(3R)ED5815
Df(2L)BSC354	Df(2R)BSC273	Df(2R)Exel6069	Df(3L)Exel6109	Df(3R)ED5938
Df(2L)BSC37	Df(2R)BSC274	Df(2R)Exel6284	Df(3L)Exel6112	Df(3R)ED6025
Df(2L)BSC454	Df(2R)BSC280	Df(2R)Exel7130	Df(3L)Exel6132	Df(3R)ED6085
Df(2L)BSC455	Df(2R)BSC281	Df(2R)Exel7149	<u>Df(3L)M21</u>	Df(3R)ED6096
Df(2L)BSC50	Df(2R)BSC298	Df(2R)Exel7162	Df(3L)ZN47	Df(3R)ED6220

Df(2L)BSC6	Df(2R)BSC303	Df(2R)Exel8057	Df(3R)10-65	Df(3R)ED6232
Df(2L)BSC688	Df(2R)BSC305	Df(2R)Kr10	Df(3R)A113	Df(3R)ED6255
Df(2L)BSC689	Df(2R)BSC307	Df(2R)M41A10	<u>Df(3R)Antp17</u>	Df(3R)ED6280
Df(2L)BSC690	Df(2R)BSC308	Df(2R)M60E	<u>Df(3R)BSC137</u>	Df(3R)ED6346
Df(2L)BSC692	Df(2R)BSC331	Df(2R)X1	Df(3R)BSC140	<u>Df(3R)ED6361</u>
Df(2L)BSC781	Df(2R)BSC347	<u>Df(2R)X58-12</u>	Df(3R)BSC141	Df(3R)ED7665
Df(2L)BSC812	Df(2R)BSC355	<u>Df(3L)1-16</u>	<u>Df(3R)BSC321</u>	Df(3R)Exel6154
Df(2L)BSC892	<u>Df(2R)BSC356</u>	Df(3L)6B-29+Df(3R)6B-29	Df(3R)BSC43	Df(3R)Exel6155
Df(2L)C144	Df(2R)BSC361	<u>Df(3L)AC1</u>	Df(3R)BSC464	Df(3R)Exel6159
Df(2L)dpp[d14]	Df(2R)BSC383	Df(3L)Aprt-32	<u>Df(3R)BSC469</u>	Df(3R)Exel6196
Df(2L)drm-P2	Df(2R)BSC425	<u>Df(3L)BSC113</u>	Df(3R)BSC47	Df(3R)Exel6197
Df(2L)ed1	Df(2R)BSC427	Df(3L)BSC117	Df(3R)BSC476	Df(3R)Exel6201
Df(2L)ED105	Df(2R)BSC429	Df(3L)BSC119	Df(3R)BSC489	Df(3R)Exel6202
<u>Df(2L)ED1102</u>	Df(2R)BSC485	Df(3L)BSC181	<u>Df(3R)BSC497</u>	Df(3R)Exel6203
Df(2L)ED1203	Df(2R)BSC550	<u>Df(3L)BSC220</u>	Df(3R)BSC501	Df(3R)Exel6264
Df(2L)ED1272	<u>Df(2R)BSC595</u>	Df(3L)BSC224	Df(3R)BSC502	Df(3R)Exel6270
Df(2L)ED1315	Df(2R)BSC597	Df(3L)BSC27	<u>Df(3R)BSC503</u>	Df(3R)Exel6272
Df(2L)ED136	Df(2R)BSC598	<u>Df(3L)BSC289</u>	Df(3R)BSC504	<u>Df(3R)Exel7328</u>
Df(2L)ED1378	Df(2R)BSC599	Df(3L)BSC368	Df(3R)BSC507	<u>Df(3R)Exel7378</u>
Df(2L)ED1473	Df(2R)BSC604	Df(3L)BSC371	Df(3R)BSC515	Df(3R)FDD-031795
Df(2L)ED19	Df(2R)BSC608	Df(3L)BSC375	Df(3R)BSC517	Df(3R)P115
Df(2L)ED247	Df(2R)BSC630	Df(3L)BSC388	<u>Df(3R)BSC547</u>	Df(3R)R133
<u>Df(2L)ED250</u>	Df(2R)BSC651	Df(3L)BSC389	<u>Df(3R)BSC549</u>	Df(3R)Tpl10
Df(2L)ED3	<u>Df(2R)BSC661</u>	Df(3L)BSC391	<u>Df(3R)BSC567</u>	Df(3R)Ubx109
Df(2L)ED334	Df(2R)BSC664	Df(3L)BSC411	<u>Df(3R)BSC619</u>	<u>Df(3R)X3F</u>
Df(2L)ED385	Df(2R)BSC701	Df(3L)BSC414	<u>Df(3R)BSC621</u>	

Deficiencies are organised in alphabetical order, and ones that generated no, few or sick progeny when crossed to the stable heteroplasmic females are underlined.

Table S2. A deficiency screen identified 38 nuclear loci carrying genes that affect mtDNA competition. Related to Figure 1.

Deficiencies	Total tested	Sick lines	<i>mt:yak</i> ≤2%	<i>mt:yak</i> ≥10%
2 nd chromosome	184	25	30	3
3 rd chromosome	155	38	3	2
Total	339	63	33	5

Table S3. A list of deficiencies that reduced *mt:yak* to ≤ 2%, increased *mt:yak* to ≥ 10%. Related to Figure 1.

Deficiency	Percent of <i>mt:yak</i>	Deficiency	Percent of <i>mt:yak</i>
<i>mt:yak</i> ≤ 2%			
Df(2L)BSC107	1.3	Df(2R)BSC280	1.85±0.32
Df(2L)BSC110	1.67±0.38	Df(2R)BSC361	1.78±0.11
Df(2L)BSC111	1.86±0.82	Df(2R)BSC383	1.44±1.23
Df(2L)BSC169	1.59±0.14	Df(2R)BSC425	1.44±0.16
Df(2L)BSC204	1.61±0.52	Df(2R)BSC597	1.60±0.55
Df(2L)BSC256	1.62±0.35	Df(2R)BSC630	1.94±0.13
Df(2L)BSC455	1.71±0.51	Df(2R)BSC769	1.55±0.26
Df(2L)BSC689	2.01±0.01	Df(2R)BSC880	1.23±0.92
Df(2L)BSC692	2.02±0.01	Df(2R)ED1725	1.11
Df(2L)ED678	1.93±0.14	Df(2R)ED1791	1.56±0.39
Df(2L)Exel6005	1.99	Df(2R)Exel6061	1.92±0.11
Df(2L)Exel7070	1.35±0.51	Df(3R)Exel6159	1.82
Df(2R)BSC267	1.64	Df(3R)Exel6264	2.00
Df(2R)BSC273	2.11±0.91	Df(3R)Exel6272	1.36
<i>mt:yak</i> ≤ 1%			
Df(2L)BSC149	0.66±0.68	Df(2R)BSC651	0.91±0.31
Df(2L)BSC240	0.03±0.03	Df(2R)BSC699	0.34±0.18
Df(2L)BSC241	0.44±0.38		
<i>mt:yak</i> ≥ 10%			
Df(2L)BSC252	29.96±3.16	Df(3R)Tpl10	12.74
Df(2L)BSC812	26.25±2.46	Df(3L)BSC730	10.14
Df(2L)C144	12.91±3.93		

All the deficiencies were tested at least twice. For those tested by three independent experiments, the percentage of *mt:yak* is presented as mean±SD.

Table S4. Primers used in this study. Related to STAR Methods.

Primers for qPCR		
Heteroplasmy line	Common primer set	Specific primer set
<i>mt:yak/mt:ND2^{del1}+CoI^{T300I}</i>	ctttaatggtaaattccattata ttattattacaatgaaaatgtaaggt	aatcatattgaacctaaaaataatg attcttgaataaatctctattaaat
<i>mt:ATP6[1]/mt:ND2^{del1}+CoI^{T300I}</i>	aattttatcagttattattggagc tcaattaatcatttagggtgaatatt	gtaaagaagtttgatttaatcc tgattctctaattattaaagatctt
<i>mt:ND2^{del1}/mt:CoI^{T300I}</i> and <i>wild-type/mt:ND2^{del1}</i>	aattttatcagttattattggagc gtaaagaagtttgatttagtcc	tcaattaatcatttaggatgaatatt tgattctctaattattaaagatctt
Primers for RT-qPCR		
Gene	Primer set	Elongation temperature
<i>Act42A</i>	caccatgaagattaagattgtg aacagagtacttgcgctc	53 °C
<i>EF1α</i>	gcgtgggttgatcagtt gatcttctccttgccatcc	60 °C
<i>tam</i>	tggaggacagggcctacag tctccaggcgattgaacatg	60 °C
<i>pol γ-β</i>	aaccgactgtcataaggt gtgtaagagcagggttg	53 °C

The mitochondrial genotype recognised by the specific primer set in each heteroplasmic line is highlighted in bold.

Supplemental References

- S1 Bratic A, Kauppila TES, Macao B, Groenke S, Siibak T, Stewart JB, et al. Complementation between polymerase- and exonuclease-deficient mitochondrial DNA polymerase mutants in genomically engineered flies. *Nat Commun* 2015;6. doi:10.1038/ncomms9808.
- S2 Samstag CL, Hoekstra JG, Huang C-H, Chaisson MJ, Youle RJ, Kennedy SR, et al. Deleterious mitochondrial DNA point mutations are overrepresented in *Drosophila* expressing a proofreading-defective DNA polymerase gamma. *PLoS Genet* 2018;14. doi:10.1371/journal.pgen.1007805.
- S3 Kaguni LS, DNA polymerase gamma, the mitochondrial replicase, *Annual Review of Biochemistry* 2004 (73):293-320